TITLE

pop-1/TCF, *ref-2/ZIC* and T-box factors regulate the development of anterior cells in the *C. elegans* embryo

AUTHORS

Jonathan D. Rumley[1], Elicia A. Preston[1], Dylan Cook[1], Felicia L. Peng[1], Amanda L. Zacharias[2, 3], Lucy Wu[1], Ilona Jileaeva[1], John Isaac Murray[1, 4]

1. **Department of Genetics, Perelman School of Medicine, University of Pennsylvania, Philadelphia, PA 19104**
2. **Division of Developmental Biology, Cincinnati Children's Hospital Medical Center, Cincinnati, OH 45229**
3. **Department of Pediatrics, University of Cincinnati College of Medicine, Cincinnati, OH 45267**
4. **Corresponding author - jmurr@pennmedicine.upenn.edu**

ABSTRACT

Patterning of the anterior-posterior axis is fundamental to animal development. The Wnt pathway plays a major role in this process by activating the expression of posterior genes in animals from worms to humans. This observation raises the question of whether the Wnt pathway or other regulators control the expression of the many anterior-expressed genes. We found that the expression of five anterior-specific genes in *Caenorhabditis elegans* embryos depends on the Wnt pathway effectors *pop-1/TCF* and *sys-1/*β-catenin. We focused further on one of these anterior genes, *ref-2/ZIC,* a conserved transcription factor expressed in multiple anterior lineages. Live imaging of *ref-2* mutant embryos identified defects in cell division timing and position in anterior lineages. *Cis*-regulatory dissection identified three *ref-2* transcriptional enhancers, one of which is necessary and sufficient for anterior-specific expression. This enhancer is activated by the T-box transcription factors TBX-37 and TBX-38, and surprisingly, concatemerized TBX-37/38 binding sites are sufficient to drive anterior-biased expression alone, despite the broad expression of TBX-37 and TBX-38. Taken together, our results highlight the diverse mechanisms used to regulate anterior expression patterns in the embryo.

INTRODUCTION

Anterior-posterior patterning regulation

Proper anterior-posterior patterning is critical for animal embryonic development and requires the Wnt pathway across all bilaterian animals from worms to humans. Typically, posterior cell

identities are induced by posteriorly-produced Wnt ligands signaling through the canonical Wnt pathway [1]. In this pathway, signal transduction in response to Wnt activates posterior-expressed gene transcription through the transcription factor TCF and its co-activator β-catenin [2]. Although this conserved role for the Wnt pathway in regulating the expression of posterior genes is well documented [3], much less is known about how genes expressed in anterior cells are regulated.

Caenorhabditis elegans has been widely used to study anterior-posterior patterning because it is genetically tractable, its embryonic lineage is invariant, and most of its developmental regulators are highly conserved in vertebrates and other animals [4–10]. Also, the majority of embryonic cell divisions are oriented along the anterior-posterior axis, and require the Wnt pathway to differentiate the two daughter fates [11–13]. Following each anterior-posterior cell division, the Wnt pathway is activated in the more posterior daughter cell, leading to high nuclear SYS-1/β-catenin and low nuclear POP-1/TCF, whereas the anterior daughter cell has low nuclear SYS-1 and high nuclear POP-1[11–13]. The combination of high nuclear SYS-1 and low nuclear POP-1 in posterior cells makes it stoichiometrically favorable for POP-1 to be bound to posterior-expressed targets as a complex with SYS-1, thereby driving their expression [14–16]. In contrast, anterior cells have low nuclear SYS-1 and high nuclear POP-1; for posterior-expressed targets, this results in POP-1 being bound in the absence of SYS-1, allowing it to recruit co-repressors, including UNC-37/groucho [17] (Figure 1A). Loss of POP-1/TCF results in posterior genes having either reduced expression in posterior cells or increased expression in anterior cells, indicative of its dual roles as an activator and repressor. Loss of SYS-1/β-catenin results only in down-regulation of posterior genes in posterior cells, consistent with an exclusive role as a posterior activator [13]. These observations leave open the question of how anterior genes are regulated in *C. elegans*.

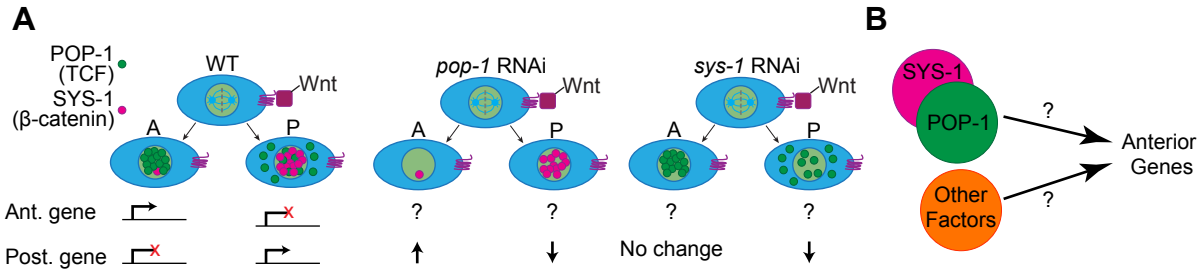

Figure 1: How are anterior genes regulated? A) The Wnt/β-catenin asymmetry pathway regulates anterior-posterior patterning by producing asymmetric nuclear concentrations of POP-1/TCF and SYS-1/β-catenin in anterior and posterior sister cells. Low nuclear concentrations of POP-1 and high nuclear concentrations of SYS-1 in the posterior cell activate expression of posterior genes and are associated with the lack of expression of anterior genes. Conversely, high nuclear concentrations of POP-1 and low nuclear concentrations of SYS-1 in the anterior cell repress posterior genes and are associated with expression of anterior genes. Effects of *pop-1* and *sys-1* RNAi on posterior genes are shown; effects on most anterior genes are unknown. B) In this work, we test whether *pop-1*/TCF and *sys-1*/β-catenin regulate anterior genes in the *C. elegans* embryo, and ask what other factors also regulate anterior expression.

Previous work suggests at least three possible mechanisms by which anterior genes could be regulated. 1) They may be regulated by the Wnt pathway indirectly, with posteriorly-expressed canonical Wnt targets repressing the expression of anterior genes in posterior cells. 2) They may be directly regulated by Wnt pathway components acting in a modified (or "opposite") manner. 3) They may be regulated by a non-Wnt-related mechanism (Figure 1B).

An example of indirect Wnt pathway regulation through a posterior repressor is seen in the *C. elegans* embryonic EMS lineage, in which cells derived from the posterior daughter of EMS, E, express the POP-1-activated, gut-specifying transcription factor *end-1*. In turn, *end-1* represses the transcription factor *ceh-51*, which is normally expressed in and specifies the lineage derived from the anterior daughter of EMS, MS [18, 19].

Conversely, the *C. elegans* anterior gene *ttx-3* is directly regulated by Wnt pathway components. *ttx-3* helps specify the AIY neuron class and is regulated by POP-1 and SYS-1 in a manner dependent on the sole *C. elegans* ZIC family transcription factor REF-2 [20]. After the AIY grandmother divides, *ttx-3* is expressed in the anterior daughter, the AIY mother, but not in the posterior daughter. In the AIY mother, the Wnt pathway is inactive, with low nuclear SYS-1 and

high nuclear POP-1, and both *pop-1* and *ref-2* are required to activate *ttx-3* expression. In its posterior sister, the Wnt pathway is active, with high nuclear SYS-1 levels and low nuclear POP-1 levels, and *sys-1* is required to repress expression of *ttx-3*. Furthermore, POP-1 and REF-2 can directly interact, suggesting that REF-2 and POP-1 bind as a complex to activate *ttx-3* expression in the AIY mother. The role of SYS-1 is less clear but some evidence suggests SYS-1 may bind to the POP-1/REF-2 complex to repress expression, or may sequester away the limited POP-1, such that POP-1 cannot interact with REF-2 [20, 21]. Similar regulation, termed "opposite Wnt regulation", has also been seen in other organisms such as *Drosophila* [22].

Because of the role of POP-1 and SYS-1 in regulating the anterior-specific expression of *ttx-3*, we hypothesized that these genes may also regulate other anterior genes. POP-1 and SYS-1 could act as general anterior expression regulators, interacting with lineage-restricted co-regulators to ensure appropriate expression of anterior genes in the correct lineages [20, 21]. We tested this by mining single-cell-resolution expression data to identify transcription factors expressed in anterior-specific patterns, and show that of five we tested, all require *pop-1* and/or *sys-1* for either anterior expression or posterior repression. We focus in more detail on a single anterior-specific gene, *ref-2/ZIC*. By automated lineage analysis of mutants we find that *ref-2* is required for normal cell division timing and cell position in *ref-2* expressing lineages. Embryonic expression of *ref-2* is driven by at least three developmental enhancers, two of which drive early embryonic expression and one of which drives expression in later-stage embryos. The most distal enhancer (3.9 kb upstream of the transcription start site) drives highly anterior-biased expression. Functional dissection revealed unexpected redundancy within this enhancer, and a role for the T-box transcription factors *tbx-37* and *tbx-38* in driving anterior-specific expression. Surprisingly, concatemers of a single T-box binding site reiterate much of the anterior-specific expression pattern of *ref-2* in early embryos, suggesting a key role for these genes in driving anterior expression.

RESULTS

Many early embryonic transcription factors have anterior-specific expression

124 We used large-scale single-cell expression databases derived from time-lapse 4D imaging of
125 embryos expressing reporter genes to identify anterior-expressed genes (Figure 2A). We define
126 "anterior" or "posterior" lineages as sets of related cells derived from either the more-anterior or
127 more-posterior daughter after a specific cell division (Figure 2B). Notably, this is distinct from
128 physical position; for example, a cell that divides near the posterior pole of the embryo gives rise
129 to both an anterior and posterior daughter lineage, both of which are located in the posterior half
130 of the embryo (Figure 2B, left side). Following convention [5, 23], all lineage trees in this
131 manuscript are drawn with the more anterior daughters on the left and the posterior daughters on
132 the right of each bifurcation. Earlier studies identified a strong tendency for genes to be expressed
133 in either multiple anterior or multiple posterior lineages during early and mid-embryogenesis;
134 these frequently appear as "lineally repetitive" patterns, with multiple related anterior or posterior
135 cousin lineages all expressing the same gene (e.g. *nob-1* and *ref-2* in Figure 2D, E) [24, 25]. Both
136 anterior-specific and posterior-specific gene expression were similarly common. While posterior
137 specific genes (e.g. Figure 2D) appear to be largely regulated by canonical Wnt signaling [13], it
138 is less clear how anterior-specific patterns are regulated. We mined existing literature and large-
139 scale databases of fluorescent reporter expression patterns (Figure 2A) [24–26] to identify 19
140 conserved genes expressed in anterior lineage-specific patterns (Figure 2C); the anterior-biased
141 expression of these genes is also seen in embryonic single-cell RNA-seq data [27].
142
143

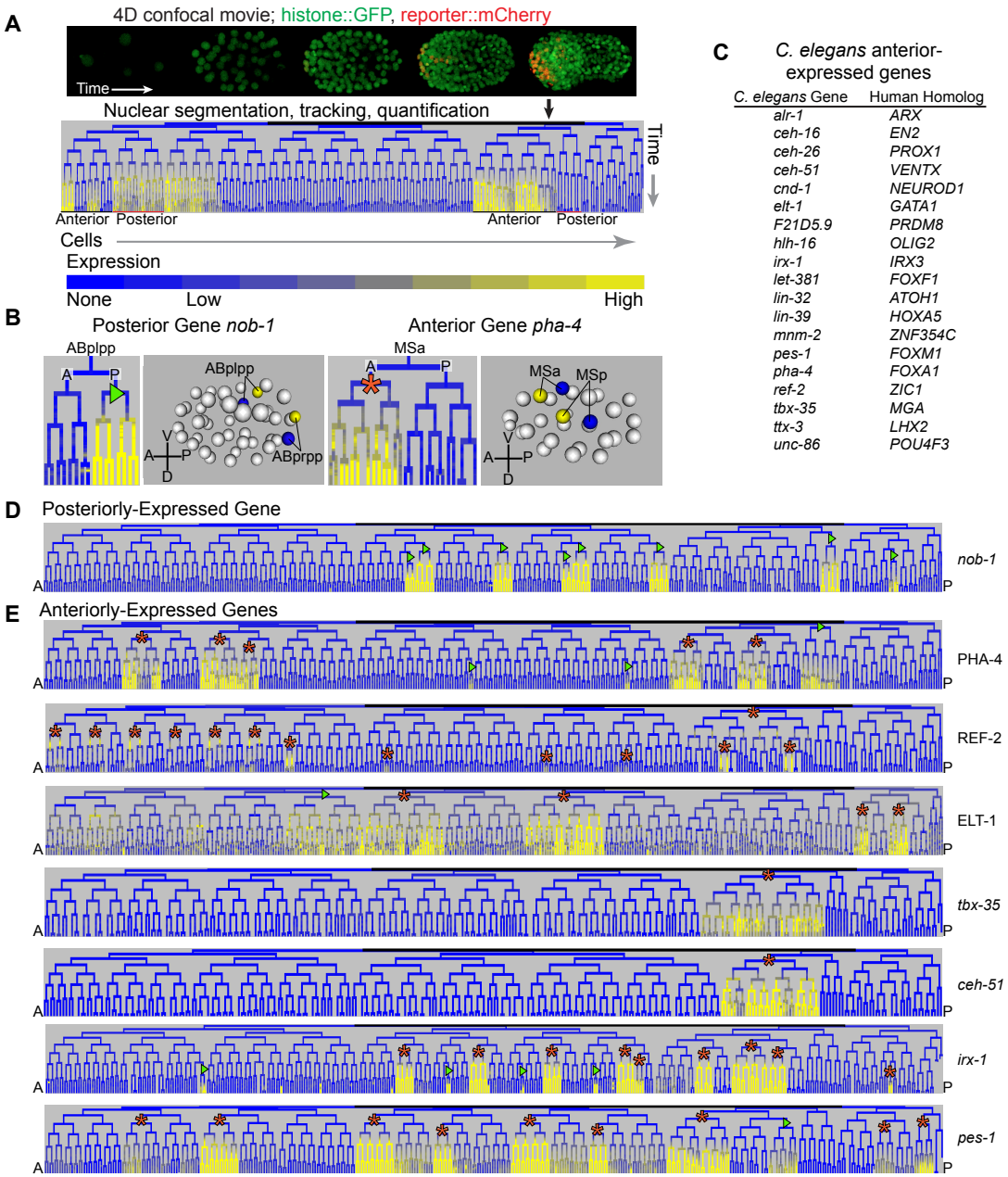

Figure 2: Identification of genes with anterior-biased expression. A) Automated lineaging traces lineages and quantifies expression from 4D confocal movies. In the lineage trees, vertical lines represent cells, and horizontal lines represent cell divisions. Most cells divide along the anterior-posterior axis, with anterior cells depicted on the left branch and posterior cells on the right branch. B) Posterior and anterior genes are denoted as such based on their expression in cells descended from either a posterior or anterior sister cell, respectively, following an anterior-posterior cell division. Anterior and posterior genes can generally be expressed in cells from any part of the embryo. Anterior and posterior founder cells are labeled with orange asterisks/green triangles respectively. C) List of anterior-biased genes in the EPiC database along with their predicted human homologs. D) Expression pattern of a posterior gene, *nob-1/Hox9-13*. E) Expression patterns of several anterior genes; most are expressed in unique combinations of mostly anterior lineages.

157 We confirmed the anterior-biased expression of seven of these by live confocal imaging followed
158 by automated cell tracking and lineage tracing (Figure 2A, E, Figure S1, Figure S2, Figure S3)
159 [26, 28]. For each gene, we collected 3D timelapse movies of transgenic embryos expressing a
160 histone-mCherry (*pha-4*, *ref-2*, *elt-1*, *tbx-35*, *irx-1*, and *pes-1*), or GFP (*ceh-51*) reporter under the
161 control of upstream regulatory sequences of each gene (referred to here as "promoter reporters").
162 For five genes we also collected images for fosmid transgenes (*irx-1, elt-1, pha-4* and *ref-2)* or
163 CRISPR knock-ins (*ceh-51*) in which the protein is fused to GFP and surrounded by its normal
164 genomic context ("protein reporters"). Each embryo also contained a ubiquitously expressed
165 second-color, histone-GFP or histone-mCherry fusion, used for cell tracking. We identified each
166 nucleus at each time point and traced them across time using StarryNite [28, 29] cell tracking
167 software, and used AceTree [30, 31] for subsequent manual error correction and validation that
168 the extracted lineages were correct. Finally, we quantified the expression of the reporter in each
169 nucleus at each time point (Figure 2A) [26]. The results confirm the anterior-specific expression
170 of each gene, and, in some cases, identify previously unknown expression patterns (Figure S1,
171 Figure S2, Figure S3). For each promoter reporter, the anterior-specific patterns were consistent,
172 but the protein fusion reporters all had additional expressing lineages and dynamics indicative of
173 distal enhancers and post-transcriptional regulation (Figure S1, Figure S2, Figure S3).
174
175 **The Wnt pathway effectors *pop-1* and *sys-1* are required for normal anterior-specific**
176 **expression**
177
178 Most genes expressed preferentially in posterior lineages require the Wnt effector transcription
179 factor POP-1/TCF either for activation in posterior cells (together with its coactivator SYS-1/β-
180 catenin) or for repression in anterior cells, and at least some are direct targets [12, 13, 32–35].
181 Although *pop-1* is required for the normal expression of some anterior genes [20, 32, 36], it is
182 unclear whether *pop-1* and *sys-1* are generally required for anterior-specific expression, as they
183 are for posterior-specific expression.
184
185 To test this, we measured the expression of five anterior gene reporters (*tbx-35*, *ceh-51*, *elt-1*, *irx-*
186 *1*, and *ref-2*) after *pop-1* and *sys-1* RNAi by live 3D imaging and lineage tracing as described
187 above. We used promoter reporters for *tbx-35*, *ceh-51*, *irx-1*, and *ref-2* because our wild-type

188 expression data indicated these reporters are sufficient for anterior regulation (Figure S1, Figure
189 S2, Figure S3). For *elt-1*, anterior-specific expression was more robust for the protein reporter so
190 we tested that reporter's dependence on *pop-1* and *sys-1* (Figure 3; Figure S4).
191
192 Reporters of two of the genes we tested, *tbx-35* and *ceh-51*, are expressed solely in the anterior
193 lineage MS (Figure S2; Figure S4A, B), and previous qualitative expression analyses indicated
194 that expression persists in the absence of *pop-1* [19, 36, 37]. Consistent with this, we detected
195 expression of both genes in the MS lineage after *pop-1* RNAi, however this expression was
196 significantly decreased. We also observed increased expression of both genes in the E lineage
197 (posterior sister of MS), although this expression remained lower than both the wild-type and *pop-*
198 *1* RNAi MS levels (Figure 3A, B; Figure S4A, B; Table S4). We also observe low-level ectopic
199 expression of *tbx-35* in the E lineage under *sys-1* RNAi. These results indicate that both *tbx-35* and
200 *ceh-51* require *pop-1* for full expression in the MS lineage and for repression in the E lineage (as
201 shown previously [19, 36]), and that *sys-1* is required to repress *tbx-35* in the E lineage.
202
203 *elt-1* reporters are expressed in several early anterior lineages that primarily give rise to ectodermal
204 fates (ABpla, ABpra, Caa and Cpa), and in one posterior lineage (ABarp) (Figure S1; Figure S4C).
205 In the Caa and Cpa lineages, anterior lineages that express both the promoter and protein reporters,
206 *pop-1* RNAi results in decreased *elt-1* reporter expression. However, RNAi for neither *pop-1* nor
207 *sys-1* affects expression in their posterior sister lineages Cap and Cpp (Figure 3C; Figure S4C;
208 Table S4). Similarly, *pop-1* RNAi results in reduced expression of the protein reporter in the ABpla
209 and ABpra lineages, while RNAi knockdown of neither *pop-1* nor *sys-1* has much effect on their
210 posterior sister lineages ABplp and ABprp (Figure S4C; Table S4). Thus, in both the ABp and C
211 lineages, *pop-1* is required for anterior expression of *elt-1*, but neither *pop-1* nor *sys-1* is required
212 for posterior repression.
213
214

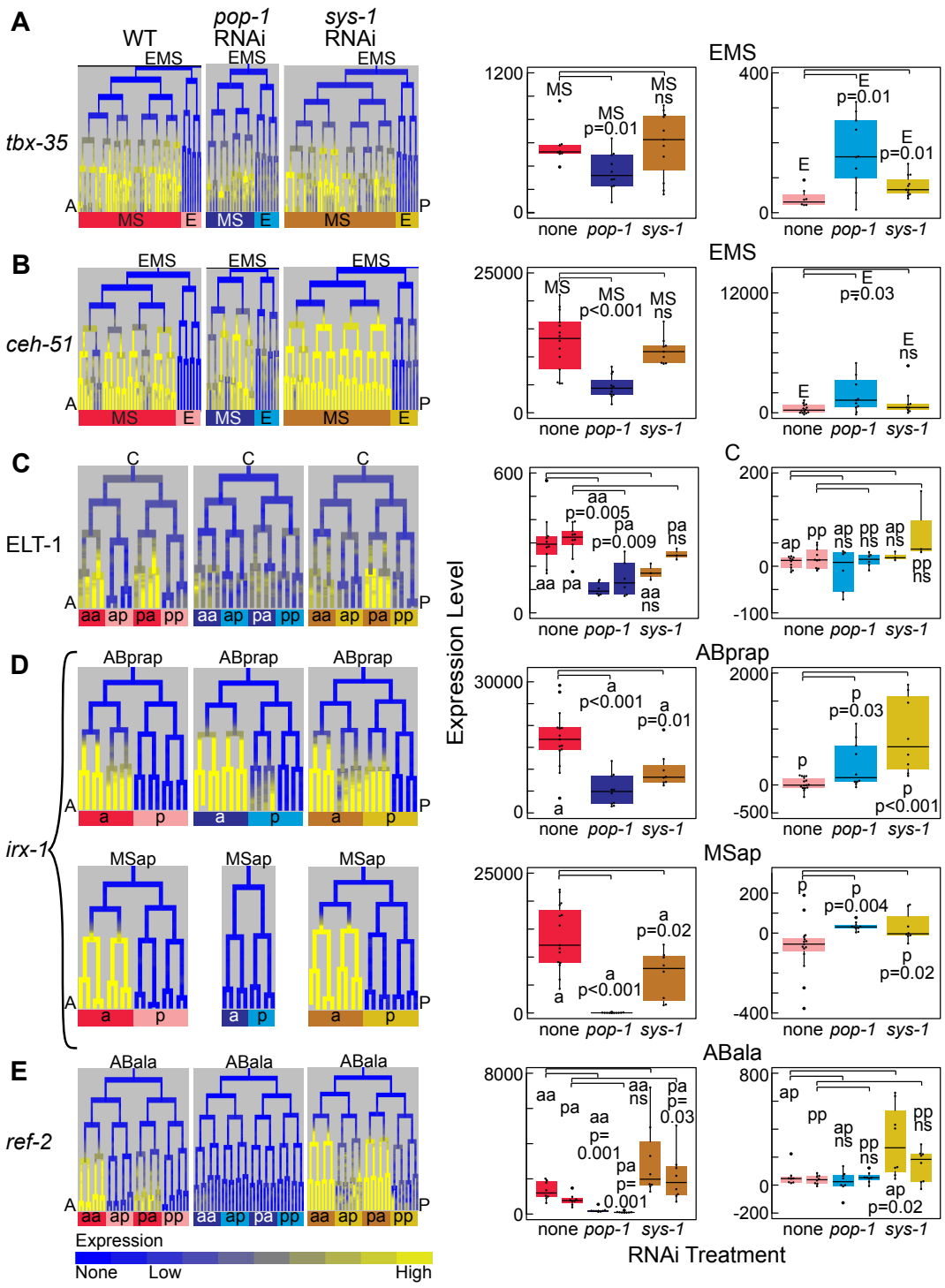

Figure 3: Regulation of anterior genes by Wnt effectors *pop-1* and *sys-1*. A-E) Expression pattern (left) and quantification (right) of reporters for the anterior genes *tbx-35* (A), *ceh-51* (B), ELT-1 (C), *irx-1* (D), and *ref-2* (E) in specific anterior lineages and their posterior sisters. Expression is shown under WT conditions and following *pop-1* or *sys-1* RNAi. Expression quantification (right) is the mean expression across all measurements within that lineage from when the reporter is normally first detected until the last time point indicated in the lineage (details in Methods).

223 *irx-1* reporters are expressed early in four related anterior sublineages of ABp, and in three anterior
224 sublineages of MS, while in later embryos they are expressed in both anterior and posterior
225 lineages (Figure S3; Figure S4D). Like for *elt-1, pop-1* RNAi reduces *irx-1* reporter expression in
226 anterior ABp-derived sublineages, and two of the MS-derived expressing sublineages lose
227 expression nearly completely. After both *pop-1* and *sys-1* RNAi, the *irx-1* reporter expression
228 expands into several posterior sublineages of ABp whose anterior sisters normally express *irx-1*
229 (Figure 3D; Figure S4D; Table S4). These results indicate that *irx-1* requires *pop-1* for expression
230 in anterior lineages and both *pop-1* and *sys-1* for repression in posterior lineages.
231
232 Reporters for *ref-2* are expressed in the early embryo in all MS descendants and in several related
233 anterior sublineages of ABa that arise at the 50-cell stage (Figure S1; Figure S4E). In later
234 embryos, expression occurs in two anterior sublineages of MS, in several anterior ABp-derived
235 sublineages, and in the Pn ventral epidermal blast cells, consistent with previous studies [38]. After
236 *pop-1* RNAi, expression of the *ref-2* promoter reporter is significantly reduced in anterior
237 sublineages of ABala (Figure 3E). As for other genes, *sys-1* RNAi caused de-repression of *ref-2*
238 in several posterior sisters of the normally expressing sublineages, but we did not detect de-
239 repression in these sublineages after *pop-1* RNAi (Figure 3E; Figure S4E; Table S4). Thus, *ref-2*
240 requires *pop-1* for expression in anterior lineages and *sys-1* for repression in posterior lineages.
241
242 To summarize these perturbations, each anterior gene tested requires *pop-1* for full expression in
243 anterior lineages. Several genes also require *pop-1* (*tbx-35*, *ceh-51* and *irx-1*) or *sys-1* (*tbx-35, irx-*
244 *1* and *ref-2*) for repression in some posterior lineages. Thus, it appears that the expression of most
245 anterior genes requires the Wnt pathway components POP-1 and SYS-1, but this dependency is
246 complex as was seen previously for posterior genes [13].
247
248 **The anterior-specific transcription factor *ref-2/ZIC* is required for normal patterns of cell**
249 **division and cell position in expressing lineages.**
250
251 The striking anterior-specific expression patterns observed for early embryonic TFs raises the
252 question of whether these factors regulate the development of anterior lineages. To address this
253 question, we focused on one anterior gene, *ref-2*. *ref-2* encodes a zinc finger transcription factor

254 homologous to mammalian ZIC genes and *Drosophila* Odd-Paired. Previous work showed that
255 *ref-2* is required to prevent "Pn" epidermal blast cells from fusing with the major hypodermal
256 syncytium in larval stages [38]. More recently, REF-2 was shown to activate the anterior-specific
257 expression of the neural regulator *ttx-3* by binding the *ttx-3 cis*-regulatory region and recruiting
258 POP-1 in a manner independent of POP-1 DNA binding activity in the AIY mother cell [20]. Since
259 *ref-2* is expressed in many other anterior lineages in early embryos, we investigated whether *ref-2*
260 mutants have developmental defects in those lineages.
261
262 We tested for embryonic lineage phenotypes at single-cell resolution by analyzing 3D time-lapse
263 movies of eight embryos homozygous for the deletion allele *ref-2(gk178)* and expressing a
264 ubiquitous histone-mCherry fusion for cell tracking. We used StarryNite to track the lineage of
265 each embryo, and used AceTree to curate the lineages through the >550-cell stage (six embryos)
266 or >350-cell stage (two embryos). We compared the position and cell cycle length of each cell in
267 each embryo to those from a reference of 17 wild-type embryos [39, 40] to identify outliers
268 ("defects") (Figure 4A).
269
270

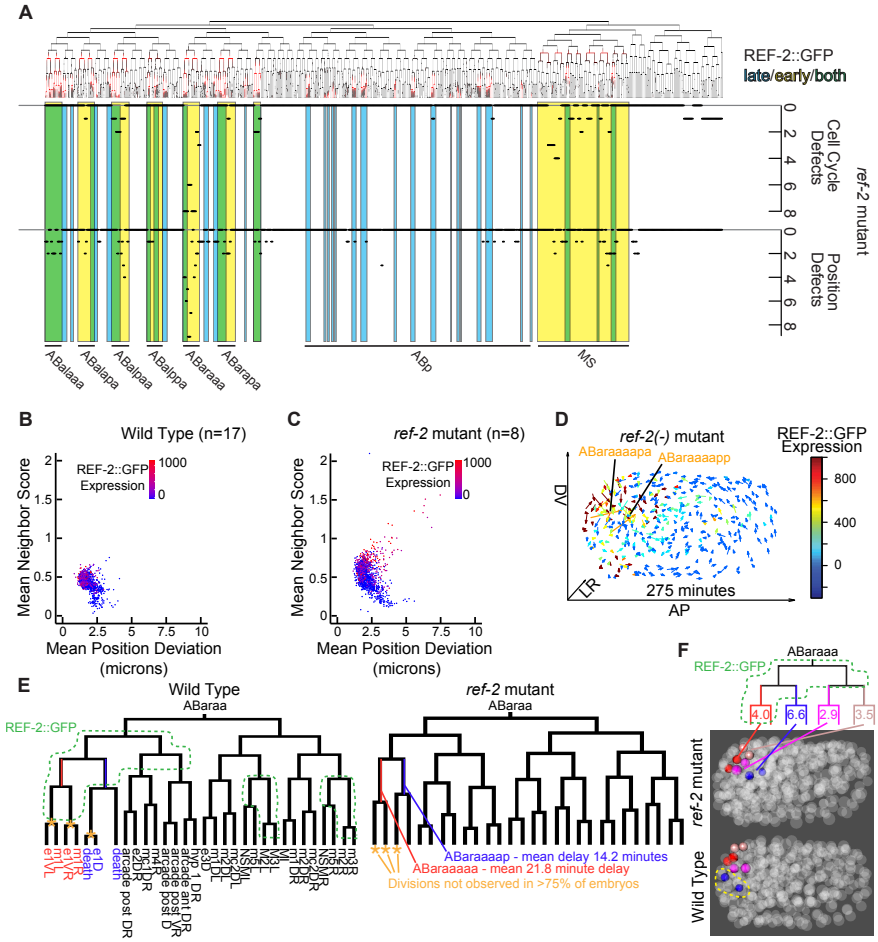

Figure 4: *ref-2* is required for proper division timing and positioning for many embryonic cells that are descended from cells that express *ref-2*. A) Lineage tree depicting the REF-2 protein expression pattern (top), and chart indicating the number of embryos out of eight homozygous *ref-2* mutant embryos that exhibit cell cycle defects and position defects in indicated cell lineages. Yellow indicates lineages that express *ref-2* early, blue indicates lineages that express *ref-2* late, and the overlap (green) indicates both. A corresponding analysis of wild-type embryos gives 0-1 defects per cell in all of 17 embryos tested [39]. B, C) Scatter plot of mean neighbor score vs mean position deviation of cells of 17 wild-type (B) and eight *ref-2* mutant (C) embryos. Neighbor score is the ratio of each cell's distances to its ten closest wild-type neighbors between mutant and wild-type embryos. Points representing cells are colored based on WT REF-2::GFP expression levels [39]. D) Plot of cell position deviations with arrows starting at the average WT position of cells and pointing to the average position in *ref-2* mutants. Arrows are colored by the WT expression levels of REF-2::GFP for each cell. The labeled cells (ABaraaaapa and ABaraaaapp) have the greatest mean cell position deviations. E) ABaraa lineages of WT and *ref-2* mutant embryos, with cells expressing REF-2::GFP outlined on the WT tree. Two delayed and three missed cell divisions are highlighted on the *ref-2* mutant tree. F) ABaraaa lineage with cells expressing REF-2::GFP outlined. The average position deviations in microns of terminal sister cells are indicated on the terminal branches of the lineage tree. Three dimensional projections of a WT and a *ref-2* mutant embryo are shown with the positions of the terminal ABaraaa lineage cells highlighted. ABaraaaapa and ABaraaaapp are outlined in the WT embryo projection as the cells with the greatest mean position deviation in the *ref-2* mutant.

293 We identified a total of 55 cells with early, late or missing divisions, and 54 of these were derived
294 from REF-2::GFP expressing lineages ($P < 10^{-15}$). Overall 95% of cell cycle defects were delays
295 or missed divisions, indicating a role for *ref-2* in promoting cell division. Similarly, we identified
296 68 position defects, of which 56 were in *ref-2* expressing lineages (Figure 4B, C, $P = 1.1 * 10^{-14}$,
297 chi-squared test). Ten *ref-2*-expressing cells, and no non-expressing cells, had position defects in
298 two or more embryos. The cells with the strongest position and cell cycle length defects were from
299 the *ref-2*-expressing anterior ABaraaa lineage, which produces primarily anterior pharynx cells
300 (e1, m1 and arcade cells). The most frequent cell cycle length defects were in ABaraaaaa and
301 ABaraaaap (both defective in 8 of 8 embryos), which were delayed by 21.8 minutes and 14.2
302 minutes, respectively (Figure 4E). The largest position defects were in ABaraaaapa and
303 ABaraaaapp, which were mispositioned on average 6 microns posterior of their wild-type position
304 (Figure 4D, F). However, other defects were broadly distributed across *ref-2*-expressing lineages,
305 in particular MS- and ABa-derived anterior sublineages (Figure 4A). In summary, the anterior
306 lineage-expressed TF *ref-2* is required for the normal development of anterior lineages, although
307 the low penetrance of many defects suggests that *ref-2* may act with other partially redundant
308 regulators, similar to other early zygotic TFs [39, 41–46].
309
310 **Modular enhancers control *ref-2* embryonic expression**
311
312 The anterior expression and phenotypes of *ref-2* raise the question of what sequences and
313 regulators control this expression. To identify genomic sequences responsible for *ref-2* anterior
314 expression, we first compared expression driven by the 31.9 kb genomic fosmid protein reporter
315 to the shorter 4.1kb upstream ("promoter") reporter (Figure 5A, B, C; Figure S6). In general, the
316 patterns were similar; both are expressed broadly in the MS lineage and in multiple anterior ABa-
317 derived sublineages. In the ABa lineage, the promoter reporter shows background expression in
318 some posterior sister sublineages suggesting the existence of repressive sequences outside of this
319 promoter region. Additionally, the promoter fusion reporter is detected persistently in both the MS
320 and AB lineages, whereas protein reporter expression is detected transiently, likely reflecting the
321 use of a stable histone-mCherry reporter for the promoter reporter. Importantly, both the REF-
322 2::GFP protein and *ref-2* promoter reporters drive expression in progenitors of most cells defective
323 in *ref-2* mutants.

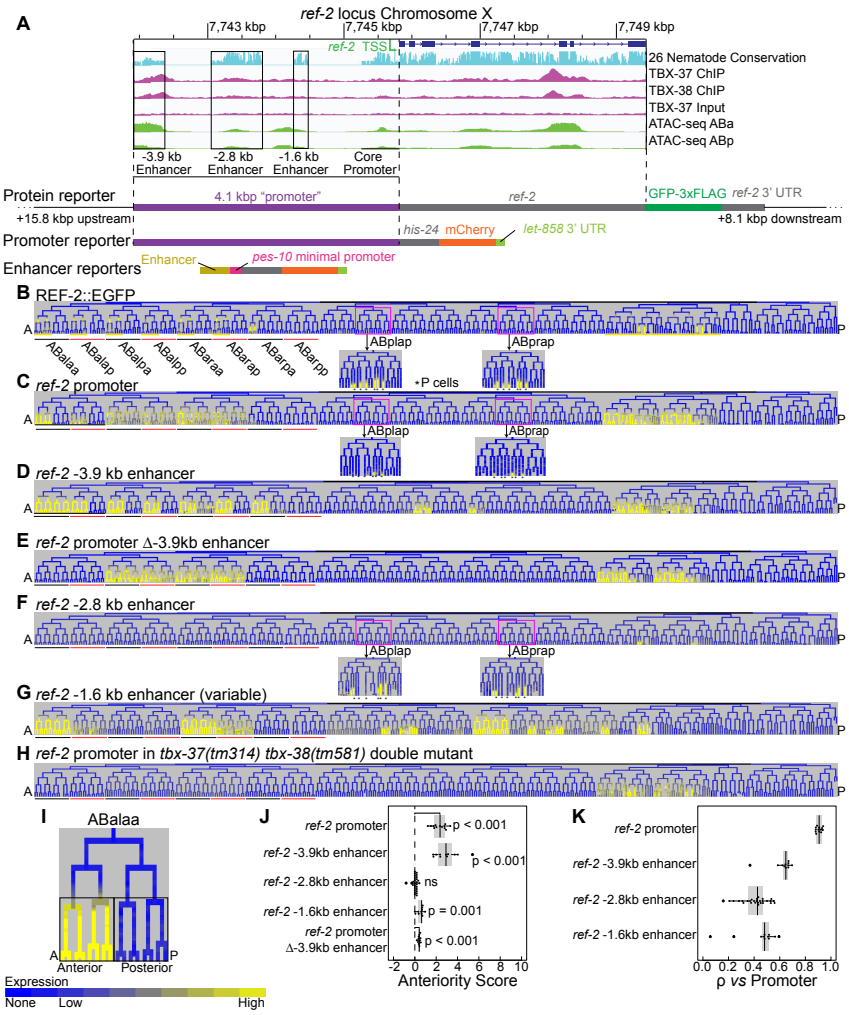

Figure 5: Identification of *ref-2* enhancers. A) Genome browser screenshot showing the *ref-2* locus on the X chromosome. Displayed tracks include the gene model, sequence conservation among 26 *Caenorhabditis* species [49], ChIP-seq data for TBX-37 and TBX-38 binding, and ATAC-seq data for cells in the ABa and ABp lineages [50]. Boxes indicate candidate enhancer regions as determined by conservation. Below the genome browser screenshot are models of the fluorescent reporter expression constructs we examined. B-H) Lineage trees showing the expression patterns of *ref-2* protein (B), promoter (C), -3.9 kb enhancer reporter (D), promoter lacking the -3.9 kb enhancer (E), -2.8 kb enhancer reporter (F), -1.6 kb enhancer reporter (G), and promoter in the *tbx-37 tbx-38* double mutant (H) as determined by time-lapse confocal microscopy. Sublineages used in anteriority analyses are labeled in B and underlined in black (anterior) and red (posterior) under each lineage tree. Sublineages with transient early REF-2::EGFP (protein reporter) expression are underlined in yellow under the lineage tree in B. Pn ventral epidermal cells are indicated with asterisks in insets of panels B, C, and F. I) Example lineage showing which cells were included in anteriority score analyses. Reporter expression levels were averaged across cells in the anterior or posterior lineages for the indicated cell generations. J) Anteriority scores of the *ref-2* promoter, enhancers, and promoter lacking the -3.9 kb enhancer. Lineages used for analysis are ABala, ABalaa, ABalap, ABalpa, ABalpp, ABaraa, ABarap, ABarpa, and ABarpp (see Figure 5B). K) Full somatic lineage correlation (Spearman's ρ) of each reporter's expression pattern with the mean expression pattern across embryos expressing the promoter reporter.

344 To identify the sequences in this region that regulate expression in these lineages, we sought to
345 identify minimal portions of the region with enhancer activity. We identified three portions of the
346 *ref-2* promoter conserved among *Caenorhabditis* species, suggesting they encode important
347 functions (Figure 5A) [47–49]. The most distal of these regions is in open chromatin in ABa-
348 derived cells as measured in a recently published ATAC-seq data set [50]. Also, this region is
349 bound by the broadly-expressed ABa lineage transcription factors TBX-37 and TBX-38, as
350 determined by a recently published ChIP-seq data set (Figure 5A) [50]. We fused each putative
351 enhancer to a reporter cassette consisting of a minimal *pes-10* promoter and a *his-24*::mCherry
352 reporter. The *pes-10* promoter is widely used, drives no consistent embryonic expression on its
353 own [13, 51, 52] and is compatible with a wide variety of enhancers [13, 51]. We introduced each
354 reporter into worms and used StarryNite to determine in which cells each putative enhancer drives
355 expression.
356
357 The most distal enhancer, located 3.9 kb upstream of the likely transcription start site, (-3.9 kb
358 enhancer; 449 base pairs) drives early expression (during gastrulation) in several anterior
359 sublineages of ABa and in anterior sublineages of MS (Figure 5D; Figure S6). This expression
360 occurs in nearly identical lineages to the early portion of the protein reporter expression pattern,
361 but while the protein reporter expression in these lineages is transient, the enhancer reporter
362 persists, again likely because of the use of a stable histone-mCherry reporter. The -3.9 kb enhancer
363 expression is also well correlated with the pattern driven by the full promoter of *ref-2* (Spearman's
364 $\rho > 0.6$, Figure 5K). Deleting this enhancer from the *ref-2* promoter reporter results in loss of the
365 strong anterior-biased expression in the ABalaa, ABalap, and ABarpa lineages, and a loss in the
366 weak anterior-biased expression in the ABalpa, ABalpp, ABaraa, and ABarap lineages. All
367 remaining consistent expression occurs in the lineages derived from the Notch-signaled cells
368 ABalp and ABara and has little anterior bias (Figure 5E, J; Figure; S5; Figure S6) [46]. The
369 significance of this expression is unclear; it can be seen in the promoter reporter but not the protein
370 reporter, suggesting that it is normally repressed by additional sequences outside the promoter. We
371 conclude that the -3.9 kb enhancer is necessary and sufficient for anterior-biased expression in the
372 ABa lineage.
373

374 A second 745 bp enhancer, located at -2.8 kb, drives expression in later embryos (bean stage) in
375 some anterior sublineages of MS and in the ABp-derived Pn ventral epidermal blast cells that were
376 previously reported to require *ref-2* [38]. These cells also robustly express the *ref-2* protein reporter
377 and weakly express the *ref-2* promoter reporter (Figure 5B, C, F, J, K). Finally, the most proximal
378 enhancer candidate (at -1.6 kb; 206 base pairs) drives variable, weakly anterior-biased, expression
379 in multiple lineages, most consistently in ABala and ABara (Figure 5G, J, K; Figure S7) and also
380 drives late expression in some ABp sublineages (Figure 5G; Figure S7). Much of this expression
381 is in cells or at stages that do not express the full-length reporters, suggesting that the activity of
382 this sequence differs in its normal genomic context.
383
384 To measure anterior expression bias, we developed an "anteriority score" based on the log2 ratio
385 between anterior and posterior sister lineage expression. Because expression tends to accumulate
386 over several cell cycles in each expressing lineage, we calculated this score based on the mean
387 expression of the progeny 2-3 cell divisions after the birth of each anterior lineage (Figure 5I).
388 Using this metric, we detected robust and significant anterior-biased expression for both the *ref-2*
389 promoter and -3.9 kb enhancer reporters in ABa-derived sublineages, and reduced or no anterior-
390 biased expression for the -2.8 kb and -1.6 kb enhancer reporters and for the promoter Δ -3.9 kb
391 enhancer reporter in the same sublineages (Figure 5J). Comparing the expression driven by each
392 enhancer to the full promoter showed each is positively, but imperfectly, correlated, consistent
393 with each driving a subset of the full pattern (Figure 5K).
394
395 ***ref-2* promoter expression requires the T-box transcription factors *tbx-37* and *tbx-38***
396
397 A dominant feature of the early *ref-2* expression pattern is reiterated expression in six of the eight
398 anterior sister cells of the ectodermal ABa lineage at the 50-cell stage (when there are 16 ABa
399 descendants). This expression is not observed in the fluorescent reporter strains until at least the
400 following cell generation (when there are 32 ABa descendants) because of the time required for
401 the fluorophores of mCherry or GFP to mature. This raises the question of whether *ref-2* expression
402 requires the ABa-specific transcription factors *tbx-37* and *tbx-38*. These genes encode redundant
403 paralogous T-box family transcription factors which are expressed throughout the ABa lineage
404 and are required for multiple cell fate decisions within ABa [44, 50, 53]. Confirming previous

405 reports [44, 50], a TBX-38::GFP knock-in reporter made by CRISPR [50] is expressed throughout
406 the ABa lineage and is detectable at least from the AB16 to AB128 stages (Figure S8). To test
407 whether *tbx-37* and *tbx-38* are necessary for *ref-2* expression, we measured expression of the *ref-*
408 *2* promoter reporter in embryos carrying homozygous deletions of both *tbx-37* and *tbx-38*. We
409 found that in the absence of *tbx-37* and *tbx-38,* nearly all *ref-2* promoter expression in the ABa
410 lineage is lost (Figure 5H; Figure S9), while expression in the MS lineage was maintained. Thus,
411 *tbx-37* and *tbx-38* are necessary for the anterior-biased expression of *ref-2* in ABa.
412
413 **The -3.9 kb enhancer contains three non-overlapping sub-enhancers that independently**
414 **drive anterior expression in the ABa lineage**
415
416 Since the *ref-2* -3.9 kb enhancer drives expression in a similar pattern to the early expression of
417 the full promoter and protein reporters, and its deletion from the *ref-2* promoter results in a
418 reduction of anterior-biased expression in portions of the ABa lineage, it is a primary enhancer
419 responsible for driving the early anterior-biased expression of *ref-2*. To map features necessary or
420 sufficient for anterior expression, we tested the activity of eight truncated versions of the *ref-2* -
421 3.9 kb enhancer to identify minimal regions of the enhancer sufficient to drive anterior expression
422 in the ABa lineage (Figure 6, Figure S10). Instead of a single minimal region, we found three non-
423 overlapping regions within the -3.9 kb enhancer that each are sufficient to drive anterior-biased
424 enhancer activity in the ABa lineage: a promoter-distal region (bases 1 to 200), a medial region
425 (bases 227 to 304) and a promoter-proximal region (bases 320 to 449) (Figure 6B, C). Of these
426 regions, the proximal region drives the most consistent expression and this expression is most
427 similar to the full length -3.9 kb enhancer construct (Figure 6D), whereas the medial and distal
428 fragments drive more variable expression and in a subset of these lineages. Thus, although
429 integration of information between these sub-enhancers is likely necessary for robustness of
430 expression pattern, the 130 bp proximal fragment provides a model system for further dissection
431 to identify anterior expression regulators.
432
433

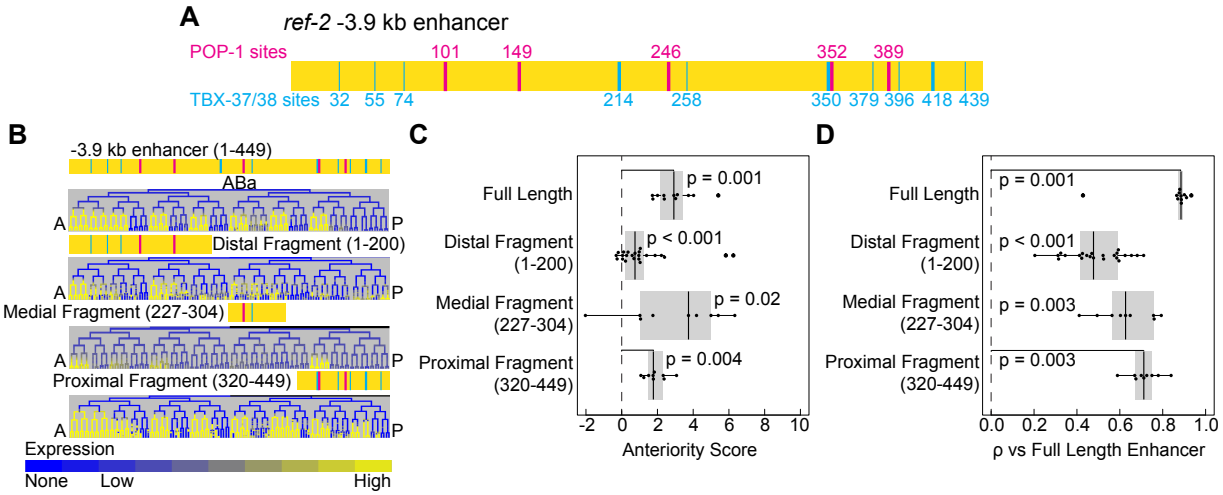

Figure 6: Three non-overlapping fragments of the -3.9 kb enhancer are each sufficient to drive anterior-biased expression in the ABa lineage of the early embryo. A) Model of the *ref-2* -3.9 kb enhancer with predicted TBX-37/38 sites (cyan, predicted high affinity sites indicated by thick line and predicted low-affinity by a thin line), and predicted high affinity POP-1 sites (magenta). B) Expression patterns driven by full-length *ref-2* -3.9 kb enhancer and by minimal fragments. C-D) Box plots displaying the anteriority scores (C) and Spearman's ρ (D) for the full-length *ref-2* -3.9 kb enhancer and minimal fragments. Lineages used to determine anteriority scores are the same as in Figure 5J. Spearman's ρ analysis uses the full ABa lineage and was calculated relative to the mean expression of the full-length -3.9 kb enhancer. A complete set of enhancer truncations tested is displayed in Figure S10.

TBX-37/38 binding sites are required for anterior expression of the proximal region

The proximal fragment exhibits broad sequence conservation with related nematodes, suggesting it contains multiple important TF binding sites (Figure 5A). To identify sequences necessary for anterior expression, we scrambled each 15 base-pair region along the length of the enhancer fragment and tested the resulting sequences for enhancer activity (Figure S11B, C, D). Scrambling a single region comprising base pairs 410-424 (coordinates relative to the full-length enhancer) resulted in a complete loss of the anterior-biased expression in the ABa lineage, indicating that this region is necessary for this expression (Figure 7B; Figure S11B). Scrambling the most proximal regions 425-439 and 435-449 resulted in a loss of expression in subsets of the ABa lineage (in ABar and ABalp) but maintained anterior expression in the ABala lineage (Figure S11B). Expression was largely maintained when other regions were mutated, suggesting sequences

459 in these regions are not individually necessary for anterior-specific expression despite their
460 conservation.
461
462 In this fragment there are five predicted TBX-37/38 sites, two of which are predicted to have high
463 affinity for TBX-37 and TBX-38. Two of the sites overlap with either the 410-424 region that is
464 essential for ABa-specific expression or the 425-449 region that is required for a subset of ABa-
465 specific expression (Figure 7A, B; Figure S11A, B). To determine whether this region is bound by
466 TBX-37 and TBX-38 *in vivo,* we mined a recently published dataset that measured genome-wide
467 TBX-37 and TBX-38 binding by ChIP-seq. Both factors show binding in the proximal region of
468 the -3.9 kb enhancer (Figure 5A) [50].
469
470 To determine whether the TBX-37/38 sites are required for anterior expression, we measured the
471 activity of the proximal fragment after mutating the two central nucleotides of all TBX-37/38 sites.
472 The mutated enhancer fragment did not drive anterior-specific expression in the ABa lineage
473 (Figure 7B, C, D; Figure S11B, C, D; Figure S12), confirming the importance of these sites.
474 Additionally, the loss of anterior-biased expression following the mutation of these sites indicates
475 that the two predicted high affinity POP-1 sites in this fragment are not sufficient to drive anterior-
476 biased expression. Also, these sites are not necessary for the anterior-biased expression driven by
477 this enhancer fragment, as the loss of these sites does not result in a loss of the anterior-biased
478 expression (Figure S11B, C, D). In fact, concatemers of POP-1 sites are sufficient to drive
479 posterior-biased expression (Figure S11F) [13, 51].
480
481 Since the high affinity site beginning at position 418 (TBX_{418}) overlaps the region (410-424)
482 required for expression, we hypothesized that this specific TBX-37/38 site may be required for
483 anterior expression in the ABa lineage. To test this, we tested the activity of the proximal fragment
484 with only the central two nucleotides of TBX_{418} mutated (Figure 7B, Figure S11B, E). This
485 mutation resulted in a loss of robust anterior-biased expression driven by the proximal fragment.
486 Therefore, TBX-37 and TBX-38 bind to the *ref-2* -3.9 kb enhancer proximal fragment and TBX_{418}
487 is necessary for it to drive robust anterior-biased expression (Figure 5A; Figure 7B, C, D; Figure
488 S11B, C, D; Figure S12), suggesting that TBX-37 and TBX-38 directly regulate *ref-2* expression.
489

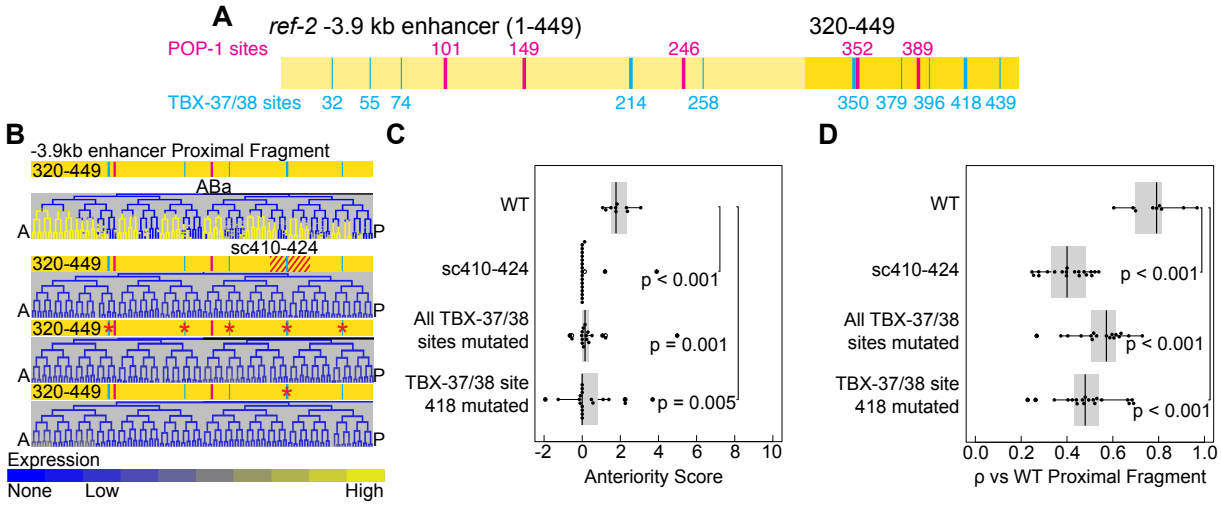

Figure 7: The ABa-expressed transcription factors *tbx-37* and *tbx-38* are required for the anterior-biased expression of *ref-2* in the ABa lineage. A) Model of the *ref-2* -3.9 kb enhancer with proximal fragment (base pairs 320-449) highlighted. Predicted TBX-37/38 and POP-1 sites are indicated as in Figure 6. B) Expression patterns driven by the WT proximal fragment of the *ref-2* -3.9 kb enhancer, with base pairs 410-424 scrambled, with all predicted TBX-37/38 sites mutated, and TBX_{418} mutated. Expression driven by the proximal fragment with additional regions scrambled or with two predicted POP-1 sites mutated are displayed in Figure S11. C-D) Anteriority scores (C) and Spearman's ρ (D) for the WT proximal fragment, with base pairs 410-424 scrambled, with all predicted TBX-37/38 sites mutated, and with TBX_{418} mutated. Lineages used to determine anteriority scores are the same as in Figure 5J. Spearman's ρ analysis uses the full ABa lineage and was calculated relative to the mean expression of the WT -3.9 kb enhancer proximal fragment.

Concatemerized TBX sites are sufficient to drive anterior-specific expression in the ABa lineage

Given that *tbx-37* and *tbx-38* are expressed in both anterior and posterior cells within the ABa lineage, we hypothesized that site TBX_{418} would be sufficient to drive broad expression in ABa, with other sequences in the enhancer required for anterior specificity. To test this, we tested the activity of synthetic enhancers comprising concatemerized copies of TBX_{418} separated by either short (6-7 bp) or long (11-15 bp) flanking sequences from its endogenous context (Figure 8A). Surprisingly, both of these reporters drove anterior-specific expression in the ABa lineage similar to that driven by the full proximal fragment (Figure 8B, C, D). This indicates that either TBX_{418} or its flanking sequences are sufficient both for ABa lineage expression, and for anterior-specific expression within this lineage. To test the possibility that the flanking sequences are responsible

517 for anterior-specificity, we scrambled those sequences while leaving the central TBX_{418} site intact
518 in the context of the long-flanking-sequence construct. The resulting reporter was again expressed
519 only in anterior sublineages similar to the full proximal fragment (Figure 8A, B, C, D). Thus, when
520 multimerized, TBX_{418} is sufficient both for ABa expression and for anterior specificity without
521 additional non-overlapping sequences.
522
523 **Anteriorly-biased expression of concatemerized TBX sites is regulated by *pop-1***
524
525 *ref-2* anterior-specific expression is dependent on *pop-1* and *sys-1*, and a concatemerized TBX-
526 37/38 binding site recapitulates part of this expression. This raises the question of whether the
527 TBX-37/38 binding site expression is *pop-1*-dependent. To test this, we examined the expression
528 of the TBX_{418} concatemer with scrambled flanking regions after *pop-1* RNAi. Knockdown of *pop-*
529 *1* results in changes in the expression pattern, including a significant decrease in anterior
530 expression bias in the ABalap lineage and a significant decrease in expression level in the ABalaa
531 lineage (Figure 8E, F, G). We also tested the expression effects of *lit-1* RNAi, which causes an
532 increase in nuclear POP-1 levels in posterior cells [16, 54, 55]. Knockdown of *lit-1* results in a
533 significant decrease in the anterior bias of the TBX_{418} concatemer expression across several
534 sublineages of ABa, including a significant increase in expression in the ABalap lineage (Figure
535 8E, F, G). Some of these changes mirror the fate transformations known to occur after *pop-1* or
536 *lit-1* RNAi, but others, including the increase in ABalap expression after *lit-1* RNAi, do not [14,
537 56]. Thus, our results indicate that either POP-1 or its targets influence both the lineage specificity
538 and anterior specificity of expression driven by TBX_{418}.
539
540
541

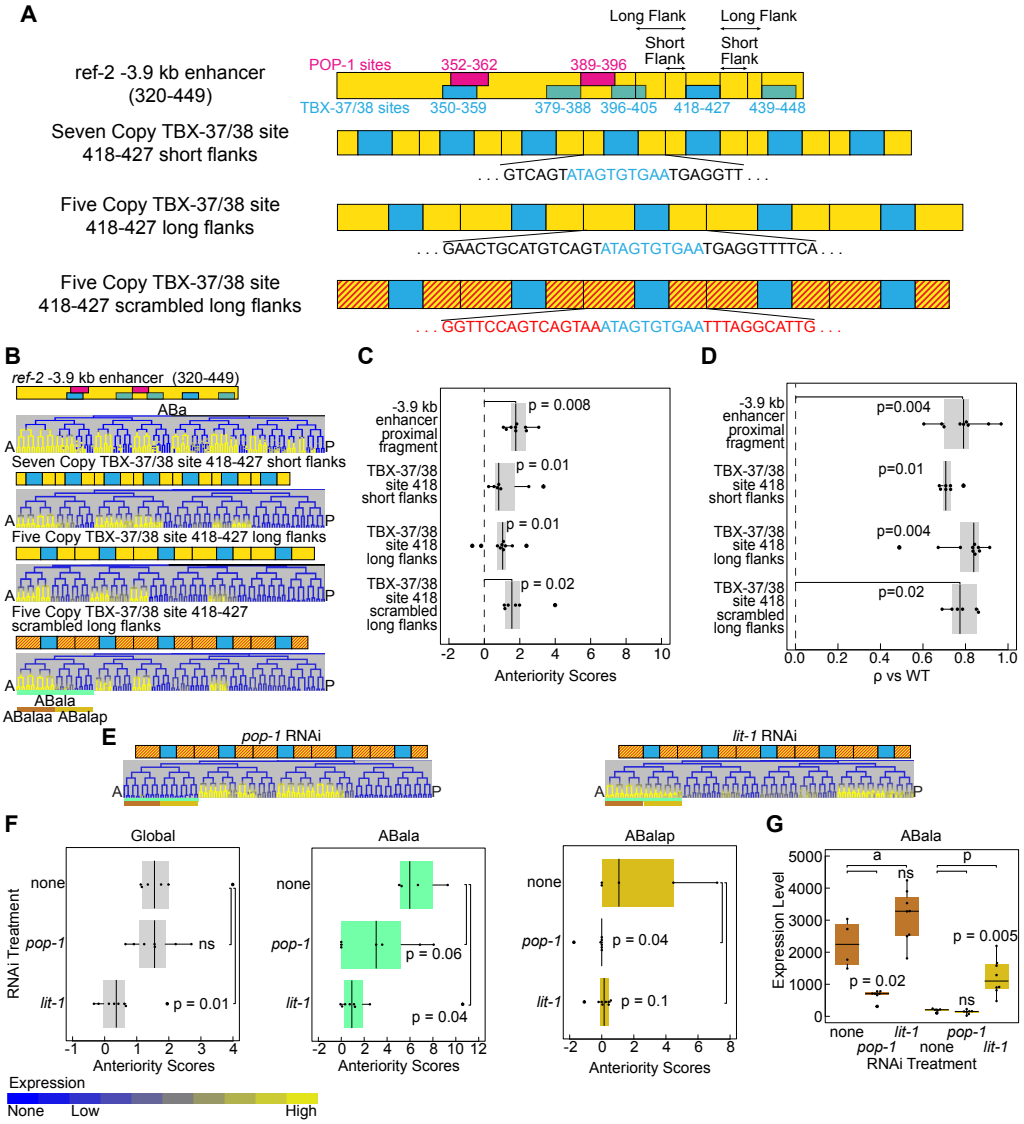

Figure 8: *TBX$_{418}$* in the *ref-2* -3.9 kb enhancer is sufficient when concatemerized to drive anterior-biased expression in the ABa lineage. A) Models of the proximal fragment of the *ref-2* -3.9 kb enhancer, the *TBX$_{418}$* seven-site concatemer with 6-7 base pair flanking regions, the *TBX$_{418}$* five-site concatemer with 11-15 base pair flanking regions, and the *TBX$_{418}$* five-site concatemer with 11-15 base pair scrambled flanking regions. B) Expression patterns driven by the proximal fragment of the *ref-2* -3.9 kb enhancer and each TBX-37/38 site concatemer. C-D) Anteriority scores (C) and Spearman's ρ (D) for the proximal fragment of the *ref-2* -3.9 kb enhancer and each TBX-37/38 binding site concatemer. E) Expression patterns driven by the *TBX$_{418}$* five-site concatemer with 11-15 base pair scrambled flanking regions after *pop-1* RNAi or *lit-1* RNAi. F) Anteriority scores for the *TBX$_{418}$* five-site concatemer with 11-15 base pair scrambled flanking regions in indicated lineages following indicated RNAi treatments. G) Quantification of reporter expression for the *TBX$_{418}$* five-site concatemer with 11-15 base pair scrambled flanking regions in the ABala lineage. Expression is shown under WT conditions and following *pop-1* or *lit-1* RNAi. Lineages used to determine global anteriority scores are the same as in Figure 5J. Spearman's ρ analysis uses the full ABa lineage expression pattern and was calculated relative to the WT proximal fragment.

559 **DISCUSSION**

560

561 Previous work has definitively shown that the Wnt pathway components POP-1 and SYS-1
562 regulate posteriorly expressed genes in the *C. elegans* embryo via the canonical Wnt asymmetry
563 pathway [12, 13, 35]. What has been less clear is how the similar number of anteriorly expressed
564 genes are regulated. We have demonstrated that a set of anteriorly expressed genes, *tbx-35*, *ceh-*
565 *51*, *elt-1*, *irx-1*, and *ref-2*, require POP-1 and SYS-1 for their anterior-biased expression. Therefore,
566 POP-1 and SYS-1 regulate the expression of anterior-biased genes. The mechanism by which
567 POP-1 and SYS-1 mediate this regulation remains to be determined. Previous work demonstrated
568 that posterior genes can be regulated by POP-1 binding directly to POP-1 binding sites in their
569 upstream regulatory regions [51]. Thus, a simple indirect model of POP-1 regulation of anterior
570 genes would be POP-1 activating the expression of repressors in posterior cells. This mechanism
571 would predict that anterior genes would be expressed later than posterior genes, or that anterior
572 genes would be expressed early in both anterior and posterior cells, but maintained only in anterior
573 cells. This can happen; for example, in the C lineage *elt-1* is expressed in both anterior and
574 posterior sister cells at the 4C stage, but is only maintained in the anterior granddaughters of C
575 (Caa and Cpa), perhaps due to its repression by the Wnt target *hlh-1* in the descendants of the
576 posterior granddaughters of C (Cap and Cpp) [32]. What we observe in many cases, however, is
577 that anterior gene expression is activated at about the same time as posterior gene expression in
578 sister lineages. This observation suggests that POP-1 could regulate some anterior genes directly.
579 Although some *pop-1* dependence of anterior genes could be explained by upstream anterior-to-
580 posterior cell fate conversions following *pop-1* RNAi, our results as a whole cannot be explained
581 by the known pattern of fate transformations [44].

582

583 Indirect *pop-1*-dependent regulation of anterior genes, however, does not explain all of its role in
584 anterior gene expression regulation. For instance, previous work showed that loss of muscle-
585 specifying TFs (MRFs) expressed in Cap and Cpp (*hlh-1*, *unc-120*, and *hnd-1*) is not sufficient to
586 permit ectopic expression of *elt-1* in these cells or to convert them to an epidermal fate [32, 57].
587 Therefore, another factor, perhaps *pop-1* acting directly, must be responsible for restricting *elt-1*
588 to the anterior C granddaughters. Our results identified a requirement for *pop-1* in anterior
589 expression of *elt-1* but not posterior repression in the C lineage. The proposed role of the MRFs in

590 repressing *elt-1* expression [32, 57, 58] suggests that this effect could partly be due to
591 misexpression of MRFs in the anterior C granddaughters, which could be tested in the future.
592
593 Direct activation of genes when Wnt is absent by POP-1/TCF, termed "opposite" Wnt target
594 regulation, occurs in other systems. For example, in *Drosophila* TCF bound directly to DNA at
595 non-optimal sites can activate transcription when unbound by β-catenin, and repress transcription
596 when bound to β-catenin. This difference in the regulatory activity of TCF is mediated by an
597 allosteric conformational change in the structure of TCF [22]. In *C. elegans*, POP-1 bound together
598 with REF-2 at the *ttx-3 cis*-regulatory region, may similarly undergo allosteric changes, leading to
599 opposite target regulation [20, 21]. Our findings are consistent with a similar mechanism regulating
600 *ref-2* itself.
601
602 Our observation that five copies of a single 10 base-pair TBX-37/38 binding site are sufficient to
603 drive anterior-biased expression in the ABa lineage suggests that a POP-1 site is likely unnecessary
604 for anterior expression. However, *tbx-37* and *tbx-38* cannot explain this anterior bias alone, as
605 these factors are expressed throughout the ABa lineage. We showed that *pop-1* is required for both
606 anterior expression and posterior repression of the *ref-2* promoter and for anterior expression of a
607 TBX-37/38 binding site concatemer. If this role of POP-1 is direct, it likely acts by binding to other
608 factors, possibly TBX-37 and TBX-38, rather than to DNA directly since the concatemer contains
609 no sequences with high affinity for POP-1. Consistent with this, TBX-38 and POP-1 were
610 previously found to physically interact with each other in a yeast 2-hybrid assay [59]. Intriguingly,
611 several other T-box factors are expressed early in the AB lineage [50, 60]; future work should
612 determine if these play a role in restricting the activity of these sites to anterior lineages. For
613 instance, TBX_{418} is predicted to be bound by several other *C. elegans* T-box factors. Other T-box
614 factors expressed in the early ABa lineage could compete for binding at this site, with POP-1
615 altering the relative activity of these factors between anterior and posterior cells. Additionally, it
616 is unclear whether *tbx-37* and *tbx-38* also regulate posterior gene expression in the ABa lineage;
617 intriguingly, the expression of *pha-4*, another anterior gene, in the ABa lineage is also dependent
618 on *tbx-37* and *tbx-38* [44].
619

620 In contrast with our observation that *TBX*$_{418}$ concatemers are sufficient to drive anterior-biased
621 expression, Murgan et al. 2015 found that a REF-2 binding site concatemer is not sufficient to
622 drive expression in the anterior AIY mother cell. Instead, Murgan et al. identified binding sites for
623 helix-loop-helix family transcription factors that are sufficient to drive expression in the AIY
624 mother and its posterior sister cell, and that combining these with REF-2 binding sites restricts
625 expression to the AIY mother. Thus, REF-2 acting through ZIC binding sites is not sufficient to
626 activate expression without cooperating factors binding other sites whereas TBX-37 and TBX-38
627 may be sufficient to do so. Other factors could also play a role, for example we used a *pes-10*
628 minimal promoter, whereas Murgan et al. did not include a minimal promoter in their constructs,
629 and there could be differences in sensitivity between the microscopy techniques [20].
630
631 Classic work in many species, including flies and vertebrates, has found that developmental genes
632 are often regulated both by partially redundant enhancers and modular enhancers that are
633 responsible for regulating distinct portions of the genes' expression patterns [61, 62]. The extent
634 to which *C. elegans* genes are regulated by such distal enhancers vs promoter proximal elements
635 has been unclear. We found that the predicted enhancers in the promoter region of *ref-2* function
636 modularly, such that each enhancer drives different expression patterns, presumably providing
637 multiple inputs to fine-tune the expression pattern of *ref-2*. Combined with other recent studies
638 this adds to evidence that enhancer-mediated regulation is widespread during *C. elegans*
639 embryonic development [52, 63–67]. Additionally, we observe modularity within the -3.9 kb
640 enhancer, with three non-overlapping regions of the enhancer each sufficient to drive anterior-
641 biased expression. Since the protein reporter is expressed in more lineages than the promoter
642 reporter, there are likely even more enhancers outside the promoter region that regulate expression
643 of *ref-2*.
644
645 Several studies have identified evidence for multiple functions of *ref-2*. *ref-2* was first identified
646 as being required for the production of the Pn.p ventral epidermal cells and for the inhibition of
647 their fusion to the epidermal syncytium hyp7 [38]. *ref-2* is also required for the initiation of the
648 differentiation of the cholinergic neuron AIY [68]. Also, *ref-2* has been found to be required for
649 female fate during sexual development [69]. We have demonstrated a role for *ref-2* in embryonic
650 development. *ref-2* is required for robust WT cell positioning and cell division timing in anterior

651 lineages. Intriguingly, an insect ortholog of *ref-2*, *odd-paired*, acts as a regulator of anterior-
652 posterior expression and is an anterior determinant in several species [70, 71], suggesting the
653 function of *ref-2* in anterior fate regulation may be ancestral. Because the defects in cell position
654 and division timing are only partially penetrant, there are likely other, partially redundant
655 regulators of cell position and cell division timing that act with the sole *C. elegans* ZIC homolog
656 *ref-2* during embryonic development. Further experiments, including suppressor and enhancer
657 screens and co-mutation of other transcription factors will need to be performed to identify other
658 factors that regulate cell position and division timing in conjunction with *ref-2*.
659
660 **METHODS**
661
662 ***C. elegans* culture and strain generation**
663
664 *C. elegans* strains (Table S1) were maintained at standard growth temperatures on OP50 *E. coli*
665 on NGM plates (Table S2). RNAi knockdown was performed by feeding, as previously described
666 [72, 73]. We validated the efficacy of *pop-1* RNAi by measuring the cell cycle delay resulting
667 from the transformation of the anterior MS lineage into an E-like lineage, the efficacy of *sys-1*
668 RNAi by failure of morphogenesis and embryonic death, and the efficacy of *lit-1* RNAi by
669 measuring the cell cycle shortening resulting from the transformation of the posterior E lineage
670 into an MS-like lineage (Table S2) [13, 33, 56]. Enhancer reporter strains were generated by
671 microinjection into RW10029, the GFP histone strain used for lineage tracing. Injection cocktails
672 consisted of reporter DNA construct at 10 ng/μL, with 5 ng/μL *myo-2*p::GFP, and 135 ng/μL
673 pBluescript vector (or highest concentration possible whenever 135 ng/μL was impossible to
674 make) and were injected using a Narishige MN-151 micromanipulator with Tritech microinjector
675 system. Other strains were created through crosses using standard approaches (Table S1).
676
677 **Generation of transgenes**
678
679 Candidate enhancers were amplified by PCR from *C. elegans* N2 strain genomic DNA with
680 Phusion HF polymerase (New England Biosciences) and gel purified (Qiagen). Enhancer
681 fragments, mutated enhancers, and binding site concatemers were ordered as either gBlocks or

682 Ultramers from Integrated DNA Technologies (Coralville, Iowa) and were amplified with Phusion
683 HF polymerase (New England Biosciences) with overhangs for stitching and either gel or PCR
684 purified (Qiagen). Enhancer reporters were produced by fusing via PCR stitching these constructs
685 to a *pes-10* minimal promoter::HIS-24::mCherry::let-858 3'UTR fragment amplified from the
686 POPTOP plasmid [51] (Addgene #34848). The enhancer reporters were purified with a PureLink
687 PCR purification kit (ThermoFisher) and/or gel purified. The desired product was determined by
688 its size based on gel electrophoresis. We identified putative transcription factor binding sites using
689 CIS-BP (http://cisbp.ccbr.utoronto.ca) [74, 75].To mutate the TBX-37/38 sites, the central two
690 nucleotides were altered (e.g. ATAG**TG**TGAA changed to ATAG**GT**TGAA for TBX_{418}). For the
691 construct with all TBX-37/38 sites mutated, after mutating the five primary sites, subsequent
692 analysis revealed two weaker sites. All of these predicted TBX-37/38 sites were mutated. The
693 reporter construct for the *ref-2* promoter lacking the -3.9 kb enhancer was amplified from N2
694 genomic DNA by PCR and PCR stitched to the *pes-10* minimal promoter::HIS-24::mCherry
695 reporter, and, thus, drives expression through the *pes-10* minimal promoter. The *pes-10* promoter
696 drives no consistent embryonic expression on its own prior to elongation [13, 51, 52] and is
697 compatible with a wide variety of enhancers [13, 51] (Table S7).
698
699 **Quantitative comparisons**
700
701 All quantitative comparisons were performed using R version 4.0.3 (The R Foundation for
702 Statistical Computing), Microsoft Excel version 16.16.27, or Python version 2.7.16. For the main
703 figures, a minimum N of 6 was used for all experiments, except for ELT-1::GFP expression after
704 *sys-1* RNAi, for which N = 3. For the supplemental figures, a minimum N of 2 was used (largely
705 for perturbations which appeared similar to wild-type at this level). Code and raw data for these
706 analyses are available at https://github.com/jisaacmurray/ref-2_paper.
707
708 *Expression and phenotypic analysis by 4D imaging*
709
710 We obtained confocal micrographs using a Leica TCS SP5 or Stellaris scanning confocal
711 microscope (67 z planes at 0.5 µm spacing and 1.5 minute time spacing, with laser power
712 increasing by 4-fold through the embryo depth to account for attenuation of signal with depth).

713 Embryos obtained from self-fertilized hermaphrodites were mounted in egg buffer/methyl
714 cellulose with 20μm beads used as spacers and imaged at 22°C using a stage temperature controller
715 (Brook Industries, Lake Villa, IL) [76]. We used StarryNite software to automatically annotate
716 nuclei and trace lineages [29]. We corrected errors from the automated analysis and quantified
717 reporter expression in each nucleus relative to the local background (using the "blot" background
718 correction technique) with AceTree software as previously described (Table S3) [24, 26].
719
720 *Anterior gene WT to RNAi within lineage comparisons*
721
722 To compare the expression levels of the anterior genes *tbx-35*, *ceh-51*, ELT-1, *irx-1*, and *ref-2* and
723 the TBX_{418} concatemer with 11-15 base pair scrambled flanking regions between WT and RNAi
724 embryos within the expressing lineages and their posterior sisters, we calculated for each embryo
725 the mean reporter expression across all measurements within each lineage (all descendant cells
726 and time points) starting with the cell stage that expresses the reporter at the time cells are born or
727 shortly afterwards to the last time point in the indicated lineage. For expression level comparisons
728 of extrachromosomal array transgenes, we normalized expression values to the 75th percentile
729 expression value of the strain with the higher 75th percentile expression value across all measured
730 cells in the indicated lineage within each RNAi treatment. The expression analyzed for the MS
731 lineage starts at an earlier stage than that for other lineages, since following *pop-1* RNAi the cell
732 divisions are so dramatically delayed that reporter expression comes on in earlier cell generations
733 in these embryos. The cell generations used in each anterior gene comparison are noted in Table
734 S4.
735
736 *Anteriority Scores*
737
738 To measure the magnitude of anterior expression bias, we developed a measure that we refer to as
739 the anteriority score. To determine the anteriority scores, first we chose a minimum expression
740 cutoff and set all values below this cutoff to 0 and subtracted the minimum cutoff from all
741 expression values greater than or equal to the cutoff (an expression value of 200 was used as the
742 cutoff for all anteriority score analyses, except a value of zero was used for the TBX-38::GFP
743 reporter, which has very low fluorescence intensity compared to the other reporters analyzed).

744 Next, we averaged the expression levels of the reporter of interest in the cells of each anterior and
745 each posterior sister lineage of interest. For the *ref-2* promoter and enhancer constructs, as well as
746 the TBX-37/38 site concatemers, we analyzed anterior and posterior lineages descended from the
747 cells ABala, ABalaa, ABalap, ABalpa ABalpp ABaraa, ABarap, ABarpa, and ABarpp. We used
748 expression values starting at the generation with ABaxxxxxx cells (AB128 stage) until the time
749 point of the last division of AB128 stage cells in the ABa lineage. Next, we calculated the means
750 of the average expression levels of all of the anterior lineages and all of the posterior lineages
751 analyzed for each embryo. We then added a pseudocount of 1 to each of the anterior and posterior
752 embryo means. For each experimental group, the adjusted average anterior expression is divided
753 by the adjusted average posterior expression, and the base 2 logarithm of the result is reported--
754 Anteriority Score = $\log_2$((anterior mean + 1)/(posterior mean +1)).
755
756 *Correlation analysis*
757
758 Correlation analysis was done by Spearman's ρ, comparing each embryo's expression to the
759 average expression of the control group. Spearman's ρ was calculated in R using the "cor"
760 function. For Spearman's ρ we used all the data from the lineages of interest without excluding
761 any cell generations or having a minimum value cutoff. We included cells born before the onset
762 of expression here to include information about the cell generation of expression onset in the
763 analysis. For the analysis comparing the *ref-2* promoter with its enhancers we used the full somatic
764 lineage starting with the blastomeres AB, EMS, C, and D. For all other analyses we used only the
765 ABa lineage.
766
767 *Mutant cell position and cell division analysis*
768
769 We identified cell position and cell cycle defects as previously described [39]. We corrected for
770 differences in global division rates, and considered divisions as defective if they deviated from the
771 wild-type cell cycle length by at least five minutes and had a z-score greater than three. Cell
772 positions were corrected for differences in embryo size and rotation, and considered defective if
773 they deviated from the expected wild type position by at least five microns, had a z-score greater
774 than five, and a nearest neighbor score greater than 0.8.

775

776 *Statistical analyses*

777

778 Statistical significance of differences in anterior or posterior expression between untreated and
779 RNAi-treated embryos was tested using the two-tailed Wilcoxon Ranked Sum test. Statistical
780 significance of differences in Spearman's ρ or Anteriority Score were tested using the one-tailed
781 Wilcoxon Ranked Sum test to test for differences from either the control group or from 0, as
782 indicated in each figure. The p-values calculated by the Wilcoxon Ranked Sum test were corrected
783 for multiple comparisons using the false discovery rate method in R. Significance of overlap
784 between positional or cell division defects and expression status were assessed using a Chi-squared
785 test.

786
787

788 **FIGURES**

789

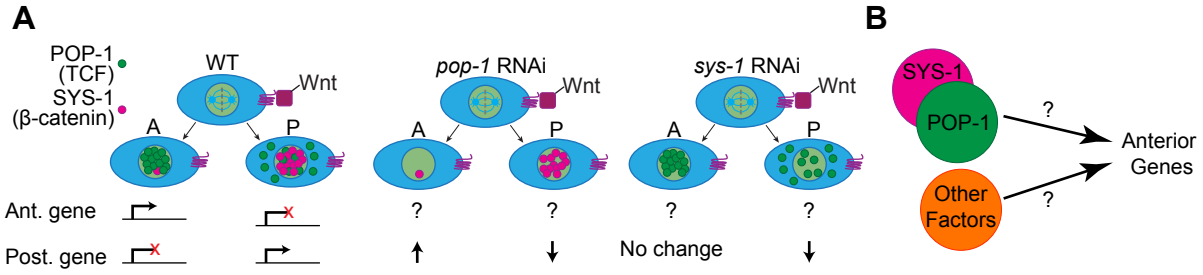

790 791 **Figure 1: How are anterior genes regulated?** A) The Wnt/β-catenin asymmetry pathway
792 regulates anterior-posterior patterning by producing asymmetric nuclear concentrations of POP-
793 1/TCF and SYS-1/β-catenin in anterior and posterior sister cells. Low nuclear concentrations of
794 POP-1 and high nuclear concentrations of SYS-1 in the posterior cell activate expression of
795 posterior genes and are associated with the lack of expression of anterior genes. Conversely, high
796 nuclear concentrations of POP-1 and low nuclear concentrations of SYS-1 in the anterior cell
797 repress posterior genes and are associated with expression of anterior genes. Effects of *pop-1* and
798 *sys-1* RNAi on posterior genes are shown; effects on most anterior genes are unknown. B) In this
799 work, we test whether *pop-1*/TCF and *sys-1*/β-catenin regulate anterior genes in the *C. elegans*
800 embryo, and ask what other factors also regulate anterior expression.

801

802

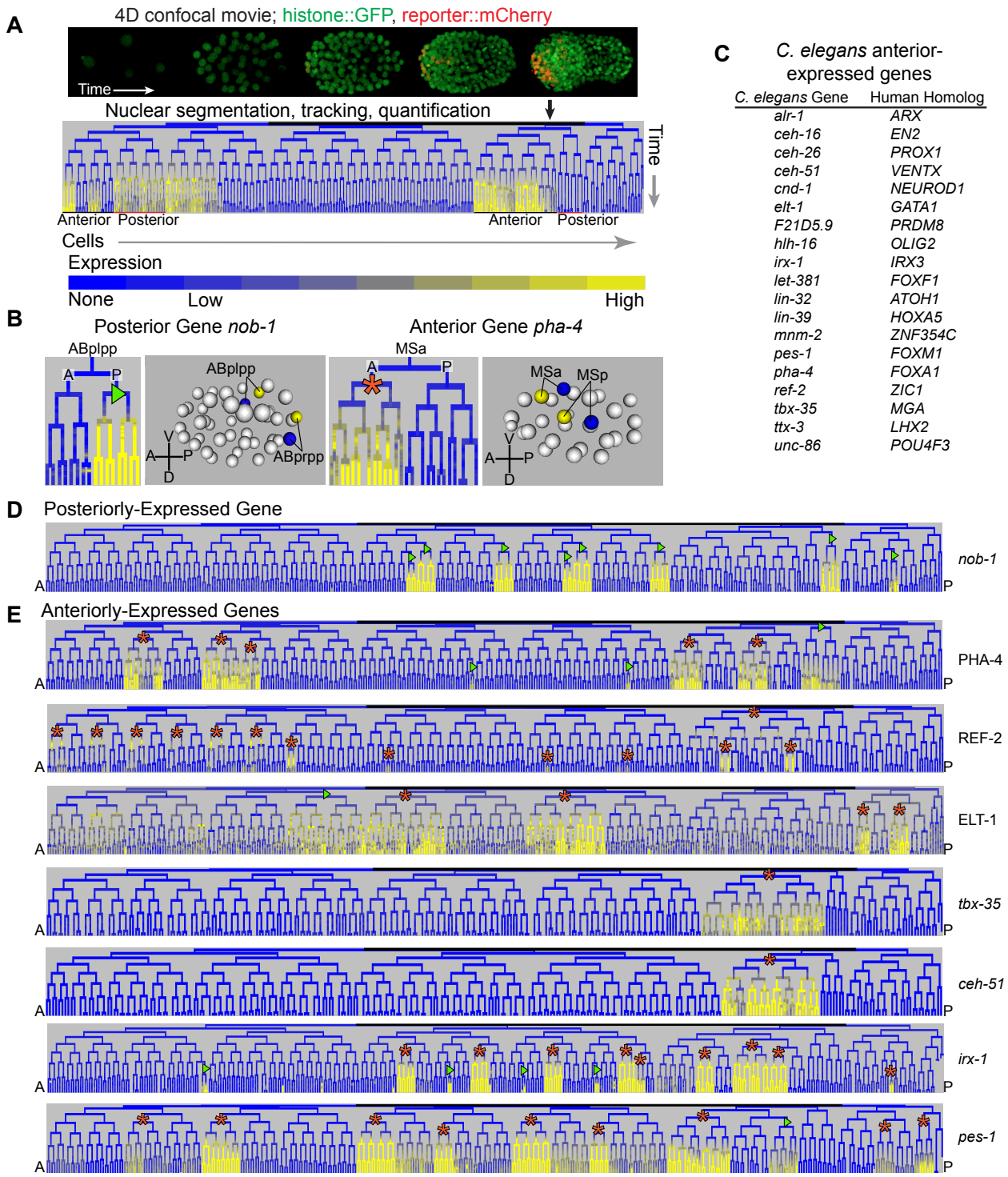

Figure 2: Identification of genes with anterior-biased expression. A) Automated lineaging traces lineages and quantifies expression from 4D confocal movies. In the lineage trees, vertical lines represent cells, and horizontal lines represent cell divisions. Most cells divide along the anterior-posterior axis, with anterior cells depicted on the left branch and posterior cells on the right branch. B) Posterior and anterior genes are denoted as such based on their expression in cells descended from either a posterior or anterior sister cell, respectively, following an anterior-posterior cell division. Anterior and posterior genes can generally be expressed in cells from any

811 part of the embryo. Anterior and posterior founder cells are labeled with orange asterisks/green
812 triangles respectively. C) List of anterior-biased genes in the EPiC database along with their
813 predicted human homologs. D) Expression pattern of a posterior gene, *nob-1/Hox9-13*. E)
814 Expression patterns of several anterior genes; most are expressed in unique combinations of mostly
815 anterior lineages.
816
817

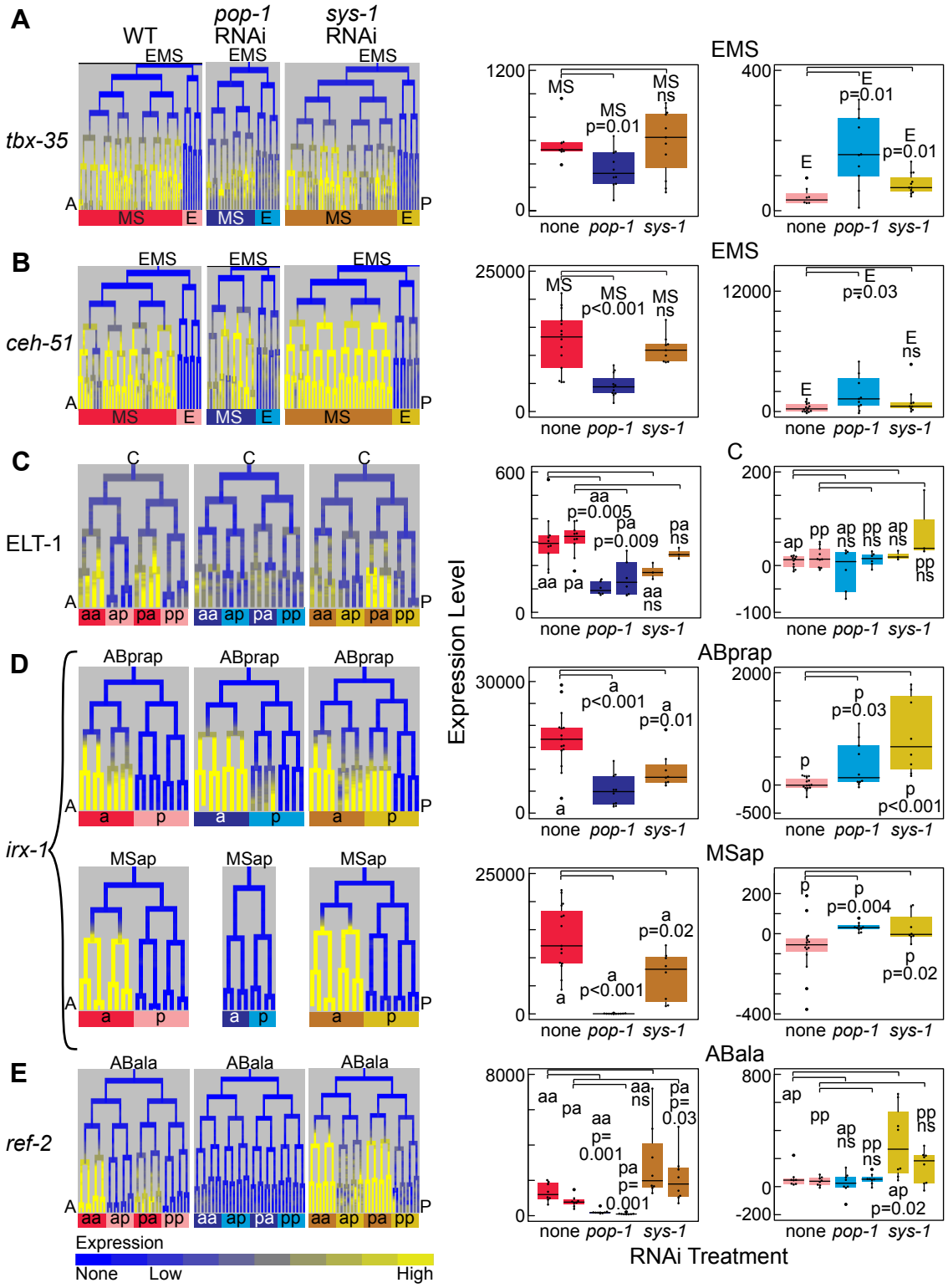

Figure 3: Regulation of anterior genes by Wnt effectors *pop-1* and *sys-1*. A-E) Expression pattern (left) and quantification (right) of reporters for the anterior genes *tbx-35* (A), *ceh-51* (B), ELT-1 (C), *irx-1* (D), and *ref-2* (E) in specific anterior lineages and their posterior sisters. Expression is shown under WT conditions and following *pop-1* or *sys-1* RNAi. Expression quantification (right) is the mean expression across all measurements within that lineage from

824 when the reporter is normally first detected until the last time point indicated in the lineage (details
825 in Methods).
826
827

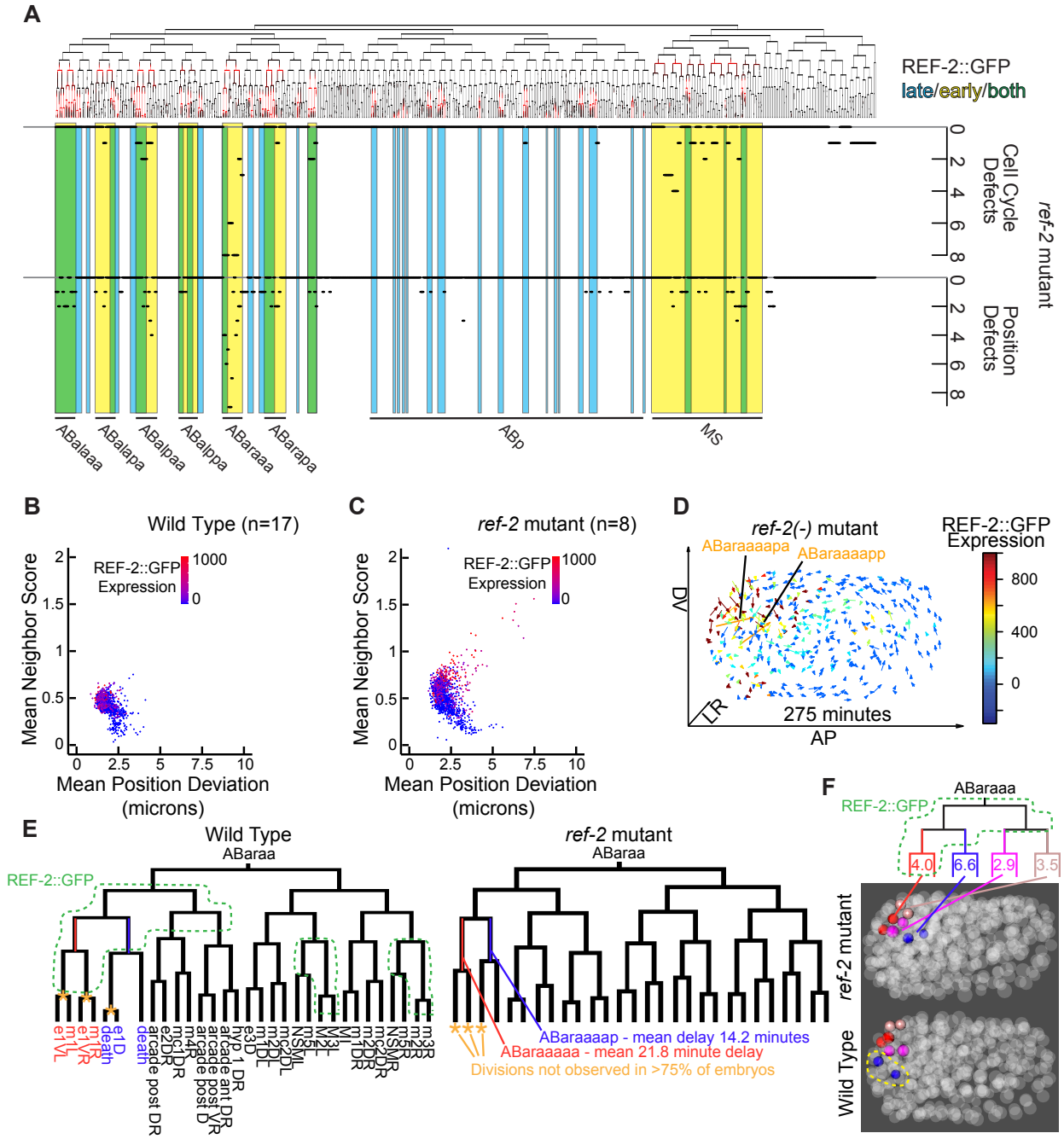

Figure 4: *ref-2* is required for proper division timing and positioning for many embryonic cells that are descended from cells that express *ref-2*. A) Lineage tree depicting the REF-2 protein expression pattern (top), and chart indicating the number of embryos out of eight homozygous *ref-2* mutant embryos that exhibit cell cycle defects and position defects in indicated cell lineages. Yellow indicates lineages that express *ref-2* early, blue indicates lineages that express *ref-2* late, and the overlap (green) indicates both. A corresponding analysis of wild-type embryos gives 0-1 defects per cell in all of 17 embryos tested [39]. B, C) Scatter plot of mean neighbor score vs mean position deviation of cells of 17 wild-type (B) and eight *ref-2* mutant (C) embryos. Neighbor score is the ratio of each cell's distances to its ten closest wild-type neighbors between mutant and wild-type embryos. Points representing cells are colored based on WT REF-2::GFP

expression levels [39]. D) Plot of cell position deviations with arrows starting at the average WT position of cells and pointing to the average position in *ref-2* mutants. Arrows are colored by the WT expression levels of REF-2::GFP for each cell. The labeled cells (ABaraaaapa and ABaraaaapp) have the greatest mean cell position deviations. E) ABaraa lineages of WT and *ref-2* mutant embryos, with cells expressing REF-2::GFP outlined on the WT tree. Two delayed and three missed cell divisions are highlighted on the *ref-2* mutant tree. F) ABaraaa lineage with cells expressing REF-2::GFP outlined. The average position deviations in microns of terminal sister cells are indicated on the terminal branches of the lineage tree. Three dimensional projections of a WT and a *ref-2* mutant embryo are shown with the positions of the terminal ABaraaa lineage cells highlighted. ABaraaaapa and ABaraaaapp are outlined in the WT embryo projection as the cells with the greatest mean position deviation in the *ref-2* mutant.

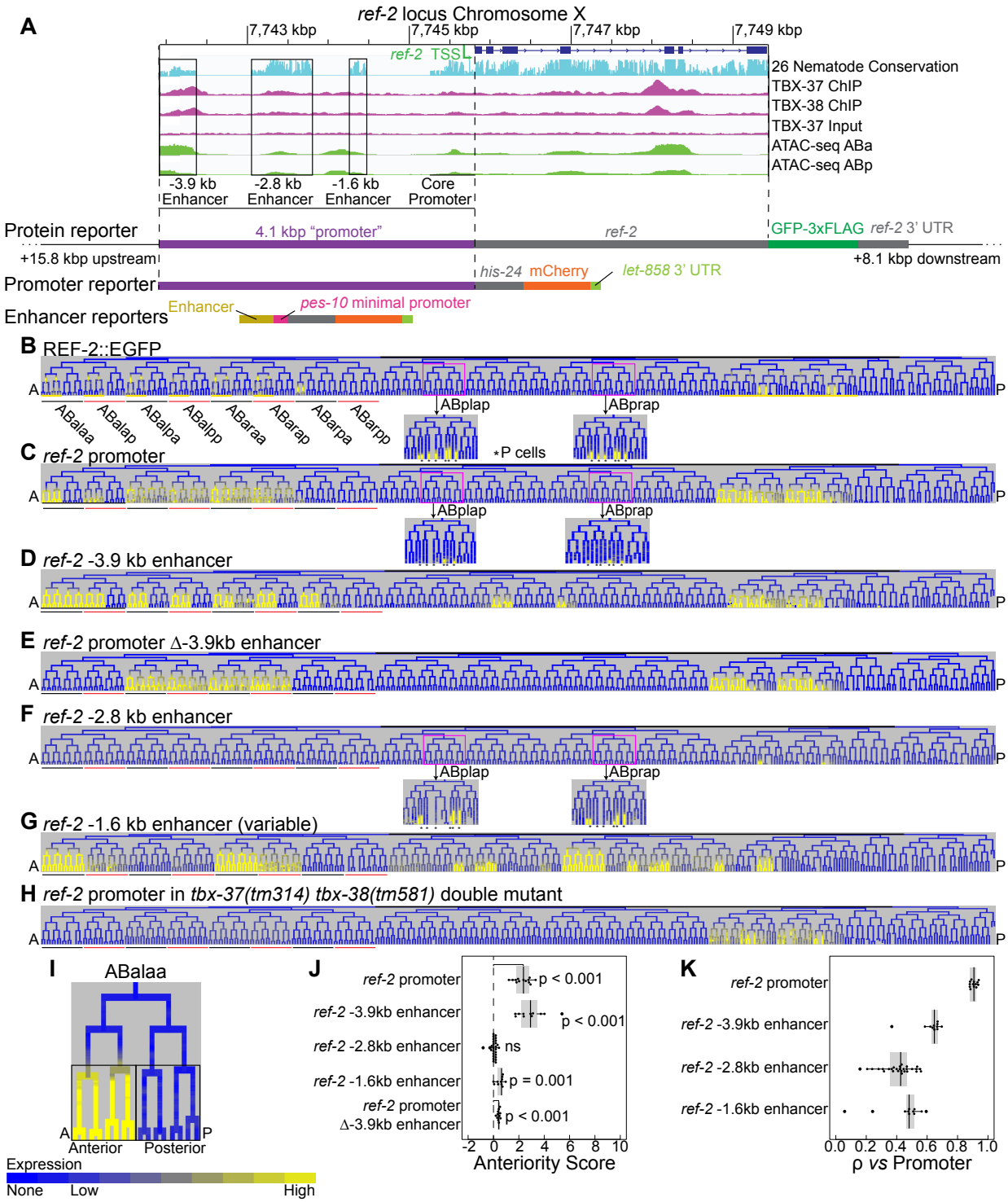

Figure 5: Identification of *ref-2* enhancers. A) Genome browser screenshot showing the *ref-2* locus on the X chromosome. Displayed tracks include the gene model, sequence conservation among 26 *Caenorhabditis* species [49], ChIP-seq data for TBX-37 and TBX-38 binding, and ATAC-seq data for cells in the ABa and ABp lineages [50]. Boxes indicate candidate enhancer regions as determined by conservation. Below the genome browser screenshot are models of the fluorescent reporter expression constructs we examined. B-H) Lineage trees showing the expression patterns of *ref-2* protein (B), promoter (C), -3.9 kb enhancer reporter (D), promoter

860 lacking the -3.9 kb enhancer (E), -2.8 kb enhancer reporter (F), -1.6 kb enhancer reporter (G), and
861 promoter in the *tbx-37 tbx-38* double mutant (H) as determined by time-lapse confocal microscopy.
862 Sublineages used in anteriority analyses are labeled in B and underlined in black (anterior) and red
863 (posterior) under each lineage tree. Sublineages with transient early REF-2::EGFP (protein
864 reporter) expression are underlined in yellow under the lineage tree in B. Pn ventral epidermal
865 cells are indicated with asterisks in insets of panels B, C, and F. I) Example lineage showing which
866 cells were included in anteriority score analyses. Reporter expression levels were averaged across
867 cells in the anterior or posterior lineages for the indicated cell generations. J) Anteriority scores of
868 the *ref-2* promoter, enhancers, and promoter lacking the -3.9 kb enhancer. Lineages used for
869 analysis are ABala, ABalaa, ABalap, ABalpa, ABalpp, ABaraa, ABarap, ABarpa, and ABarpp
870 (see Figure 5B). K) Full somatic lineage correlation (Spearman's ρ) of each reporter's expression
871 pattern with the mean expression pattern across embryos expressing the promoter reporter.
872
873

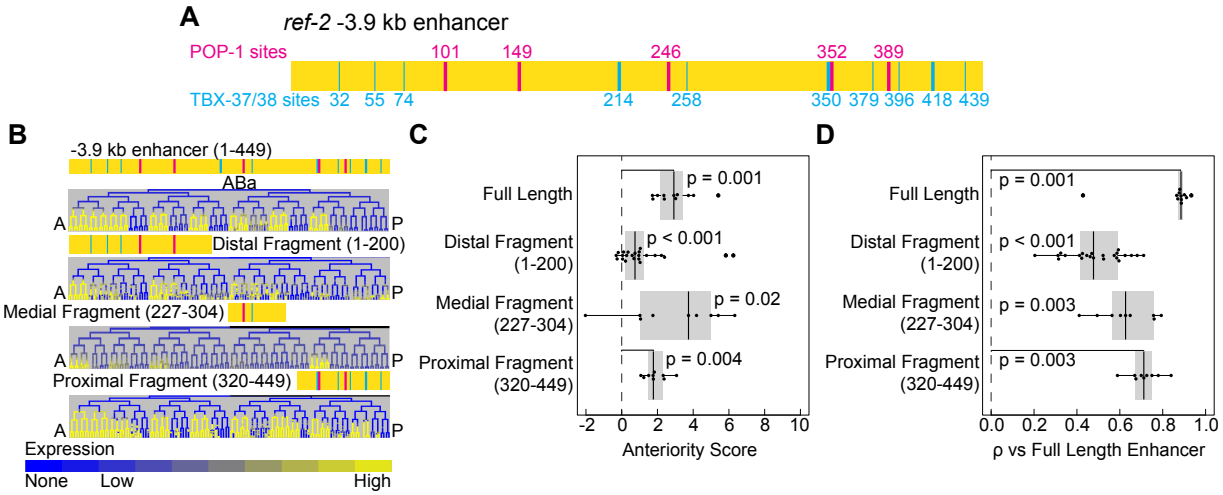

Figure 6: Three non-overlapping fragments of the -3.9 kb enhancer are each sufficient to drive anterior-biased expression in the ABa lineage of the early embryo. A) Model of the *ref-2* -3.9 kb enhancer with predicted TBX-37/38 sites (cyan, predicted high affinity sites indicated by thick line and predicted low-affinity by a thin line), and predicted high affinity POP-1 sites (magenta). B) Expression patterns driven by full-length *ref-2* -3.9 kb enhancer and by minimal fragments. C-D) Box plots displaying the anteriority scores (C) and Spearman's ρ (D) for the full-length *ref-2* -3.9 kb enhancer and minimal fragments. Lineages used to determine anteriority scores are the same as in Figure 5J. Spearman's ρ analysis uses the full ABa lineage and was calculated relative to the mean expression of the full-length -3.9 kb enhancer. A complete set of enhancer truncations tested is displayed in Figure S10.

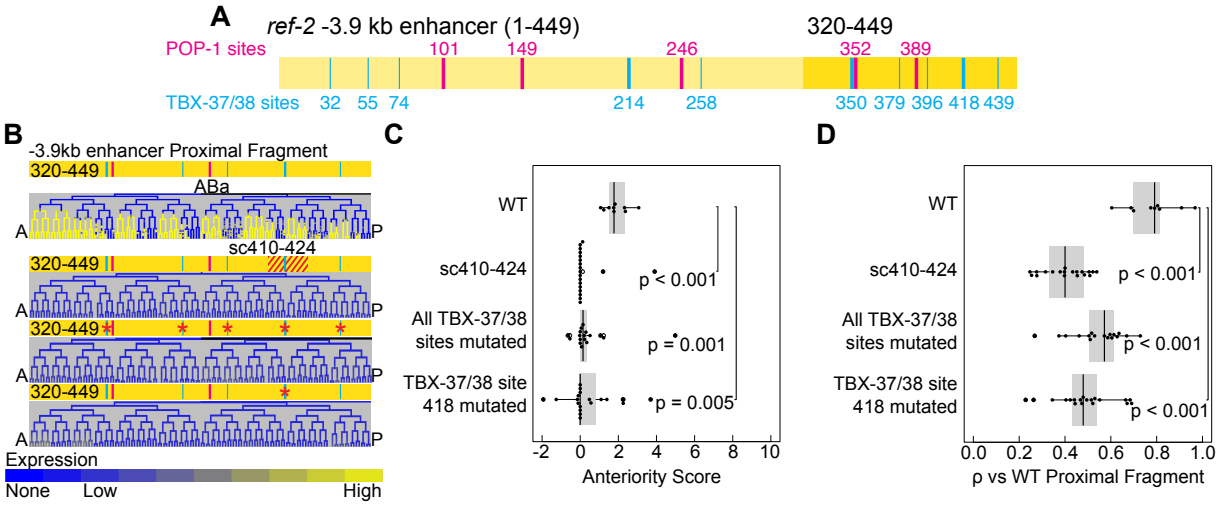

Figure 7: The ABa-expressed transcription factors *tbx-37* and *tbx-38* are required for the anterior-biased expression of *ref-2* in the ABa lineage. A) Model of the *ref-2* -3.9 kb enhancer with proximal fragment (base pairs 320-449) highlighted. Predicted TBX-37/38 and POP-1 sites are indicated as in Figure 6. B) Expression patterns driven by the WT proximal fragment of the *ref-2* -3.9 kb enhancer, with base pairs 410-424 scrambled, with all predicted TBX-37/38 sites mutated, and TBX_{418} mutated. Expression driven by the proximal fragment with additional regions scrambled or with two predicted POP-1 sites mutated are displayed in Figure S11. C-D) Anteriority scores (C) and Spearman's ρ (D) for the WT proximal fragment, with base pairs 410-424 scrambled, with all predicted TBX-37/38 sites mutated, and with TBX_{418} mutated. Lineages used to determine anteriority scores are the same as in Figure 5J. Spearman's ρ analysis uses the full ABa lineage and was calculated relative to the mean expression of the WT -3.9 kb enhancer proximal fragment.

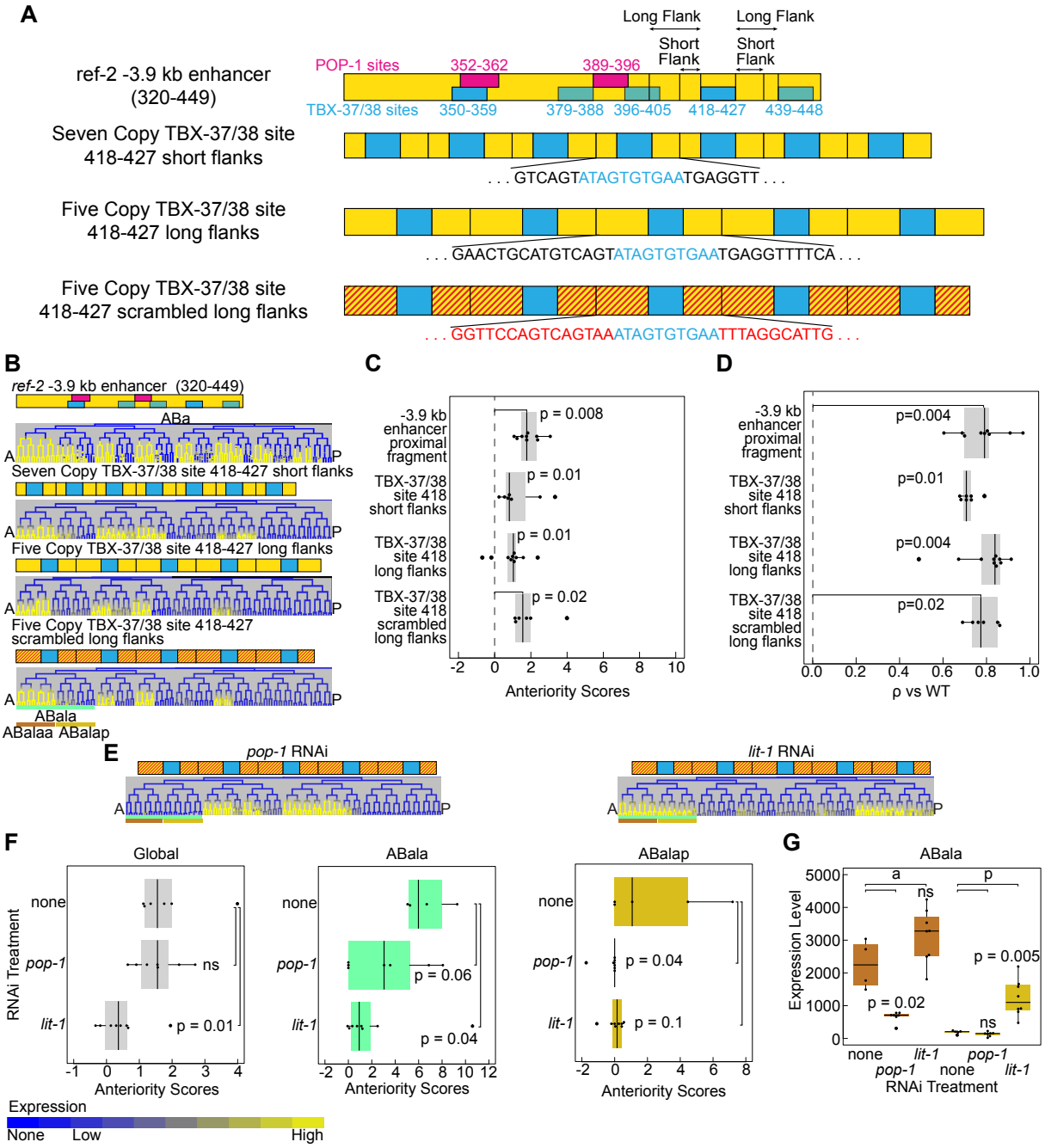

Figure 8: *TBX$_{418}$* in the *ref-2* -3.9 kb enhancer is sufficient when concatemerized to drive anterior-biased expression in the ABa lineage. A) Models of the proximal fragment of the *ref-2* -3.9 kb enhancer, the *TBX$_{418}$* seven-site concatemer with 6-7 base pair flanking regions, the *TBX$_{418}$* five-site concatemer with 11-15 base pair flanking regions, and the *TBX$_{418}$* five-site concatemer with 11-15 base pair scrambled flanking regions. B) Expression patterns driven by the proximal fragment of the *ref-2* -3.9 kb enhancer and each TBX-37/38 site concatemer. C-D) Anteriority scores (C) and Spearman's ρ (D) for the proximal fragment of the *ref-2* -3.9 kb enhancer and each TBX-37/38 binding site concatemer. E) Expression patterns driven by the *TBX$_{418}$* five-site concatemer with 11-15 base pair scrambled flanking regions after *pop-1* RNAi or *lit-1* RNAi. F) Anteriority scores for the *TBX$_{418}$* five-site concatemer with 11-15 base pair

913 scrambled flanking regions in indicated lineages following indicated RNAi treatments. G)
914 Quantification of reporter expression for the *TBX*$_{418}$ five-site concatemer with 11-15 base pair
915 scrambled flanking regions in the ABala lineage. Expression is shown under WT conditions and
916 following *pop-1* or *lit-1* RNAi. Lineages used to determine global anteriority scores are the same
917 as in Figure 5J. Spearman's ρ analysis uses the full ABa lineage expression pattern and was
918 calculated relative to the WT proximal fragment.
919
920

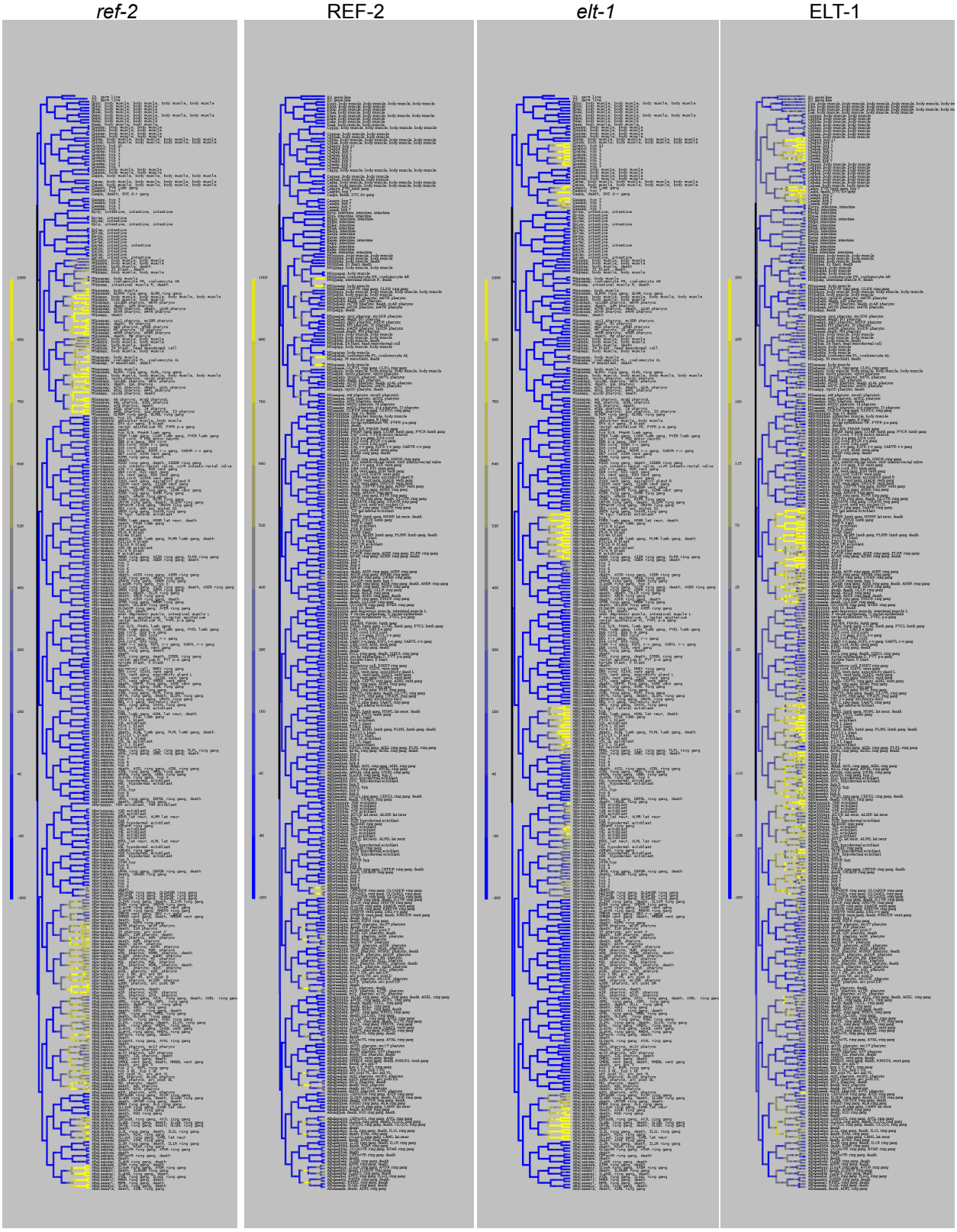

Figure S1: Several early embryonic genes are expressed with anterior bias. Full lineage expression patterns are shown for integrated transgenic promoter reporters of *ref-2* and *elt-1*; and for integrated transgenic protein reporters of REF-2 and ELT-1.

tbx-35 *ceh-51* CEH-51 PHA-4

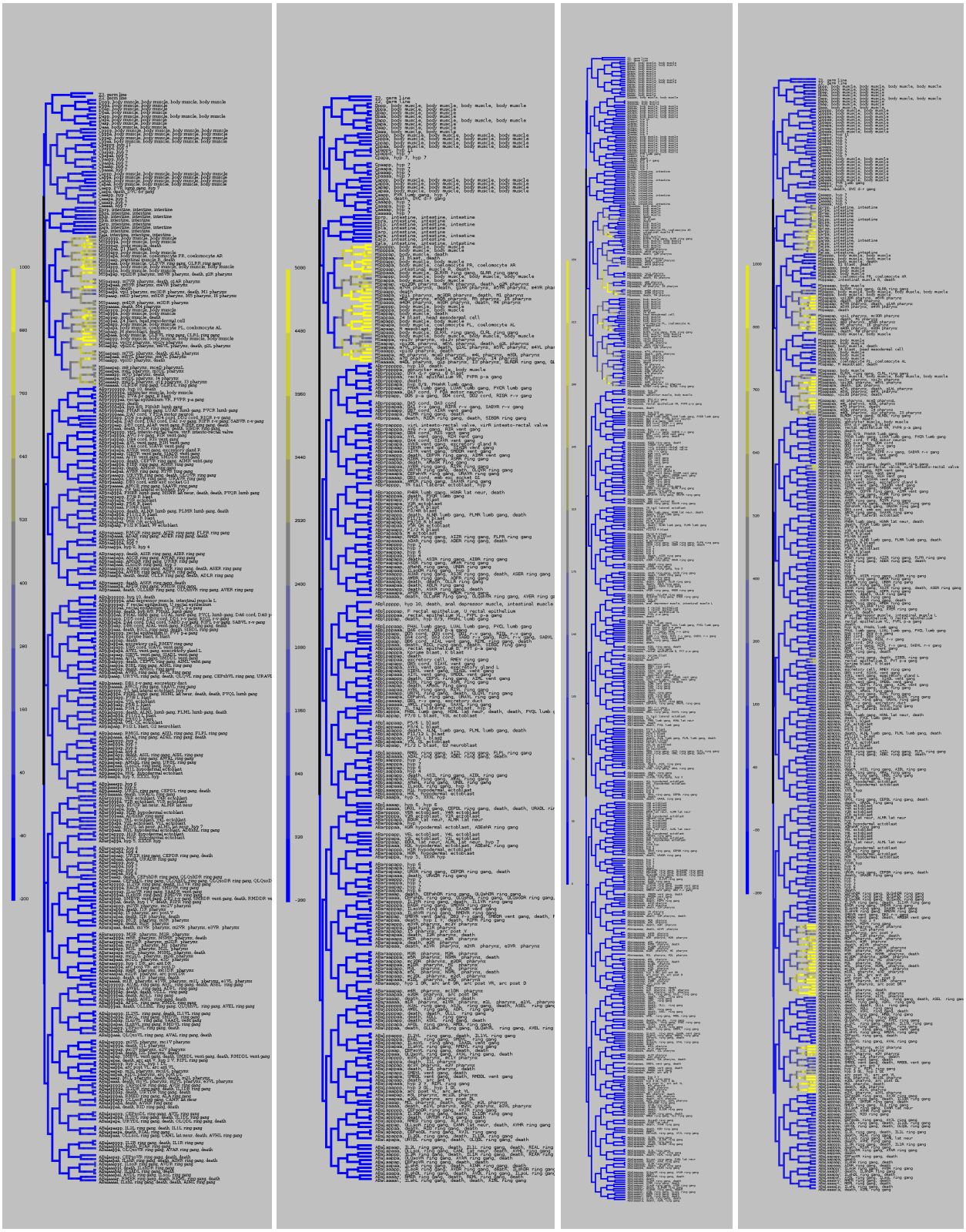

925
926
927

928 **Figure S2: Several early embryonic genes are expressed with anterior bias.**
929 Full lineage expression patterns are shown for integrated transgenic promoter reporters of *tbx-35*
930 and *ceh-51*; for an integrated transgenic protein reporter of PHA-4; and for a CRISPR knock-in
931 protein reporter of CEH-51.
932
933

irx-1 IRX-1 *pes-1*

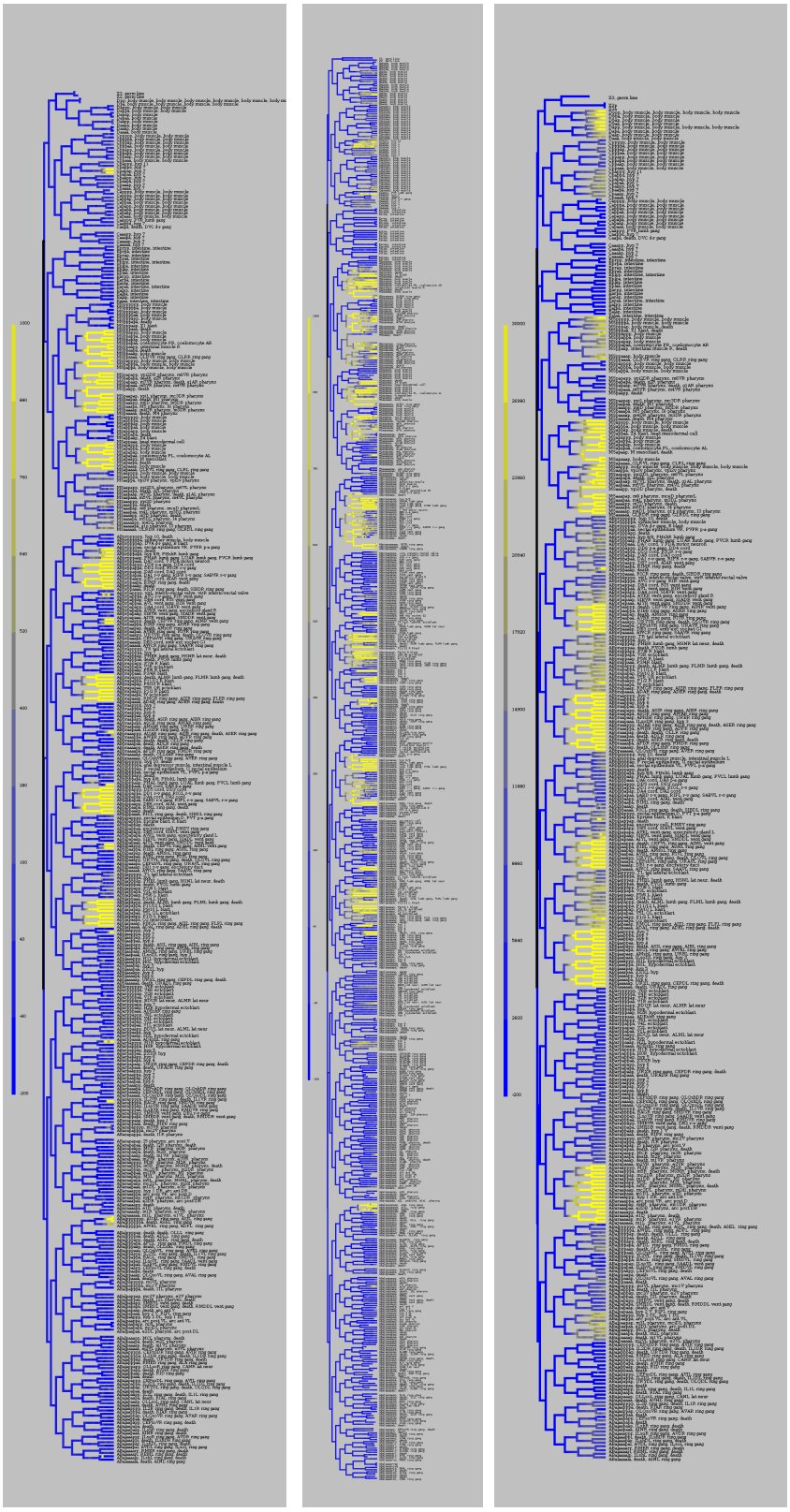

934
935
936

937 **Figure S3: Several early embryonic genes are expressed with anterior bias.**
938 Full lineage expression patterns are shown for integrated transgenic promoter reporters of *irx-1*
939 and *pes-1*; and for an integrated transgenic protein reporter of IRX-1.

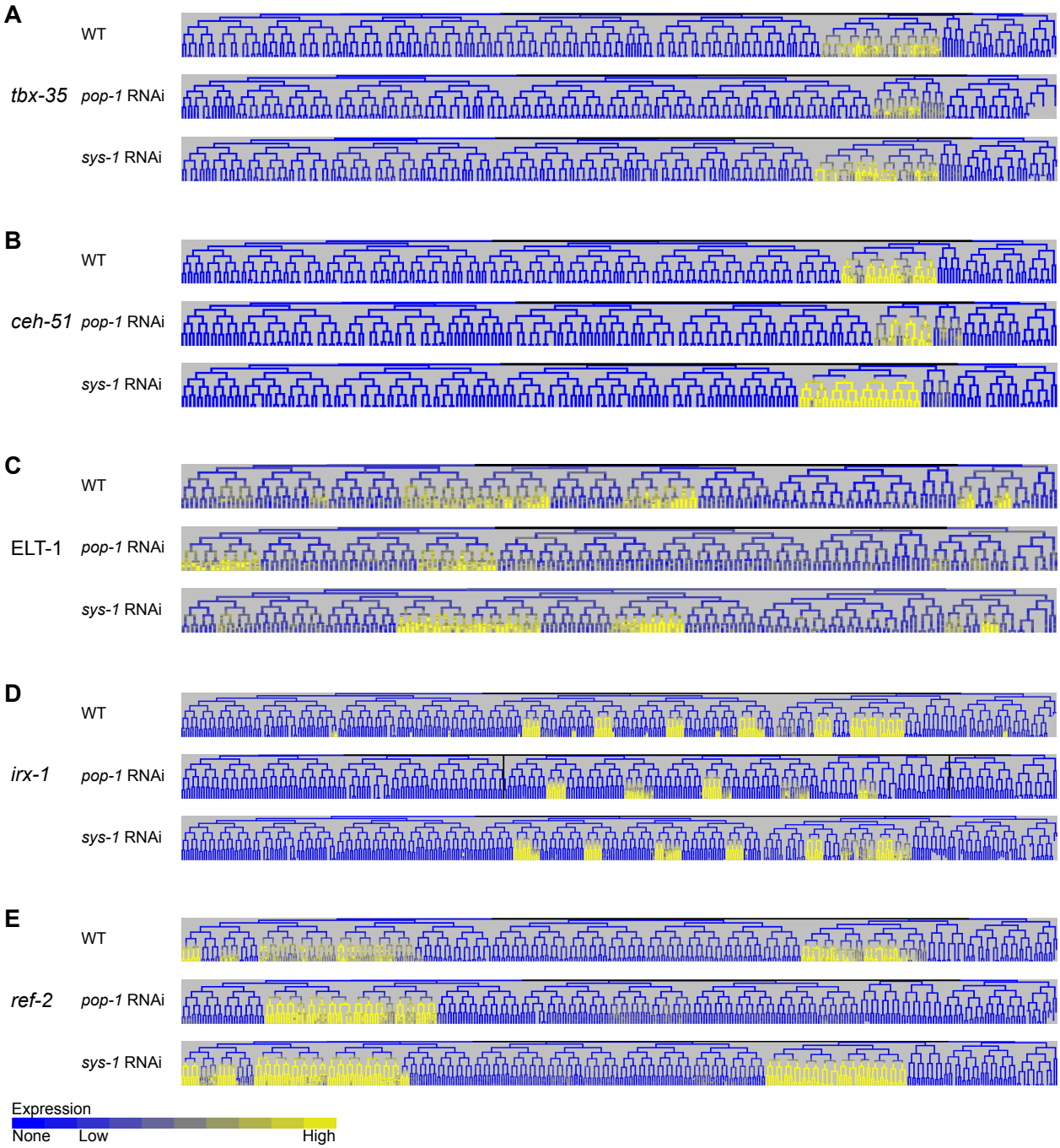

Figure S4: Anterior genes are regulated by Wnt effectors *pop-1* and *sys-1*. Full example WT, *pop-1* RNAi, and *sys-1* RNAi lineages are shown for integrated transgenic promoter reporters of *tbx-35* (A), *ceh-51* (B), *irx-1* (D), and *ref-2* (E) and for an integrated transgenic protein reporter of ELT-1 (C).

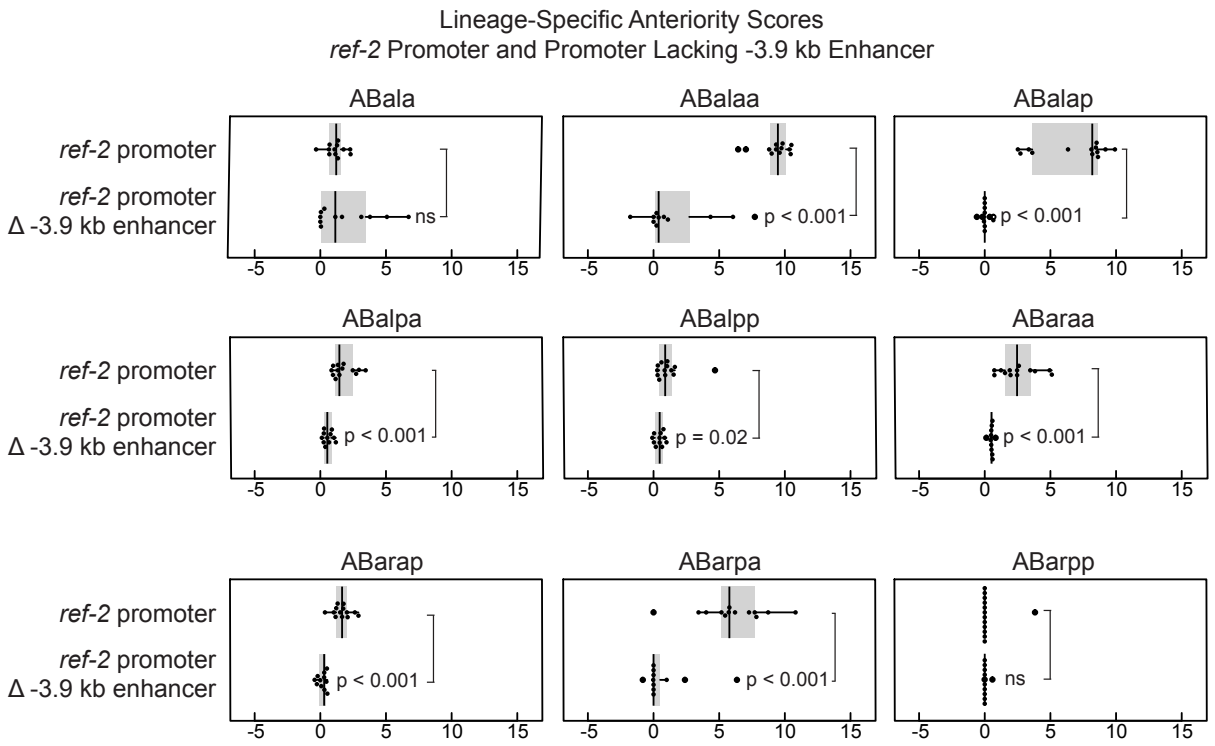

Figure S5: Deletion of the -3.9 kb enhancer from the *ref-2* promoter causes a reduction in the anterior bias in the expression driven by the promoter in most ABa sublineages in which the full-length promoter drives anterior-biased expression. Box plots display anteriority scores of lineages descended from indicated cells.

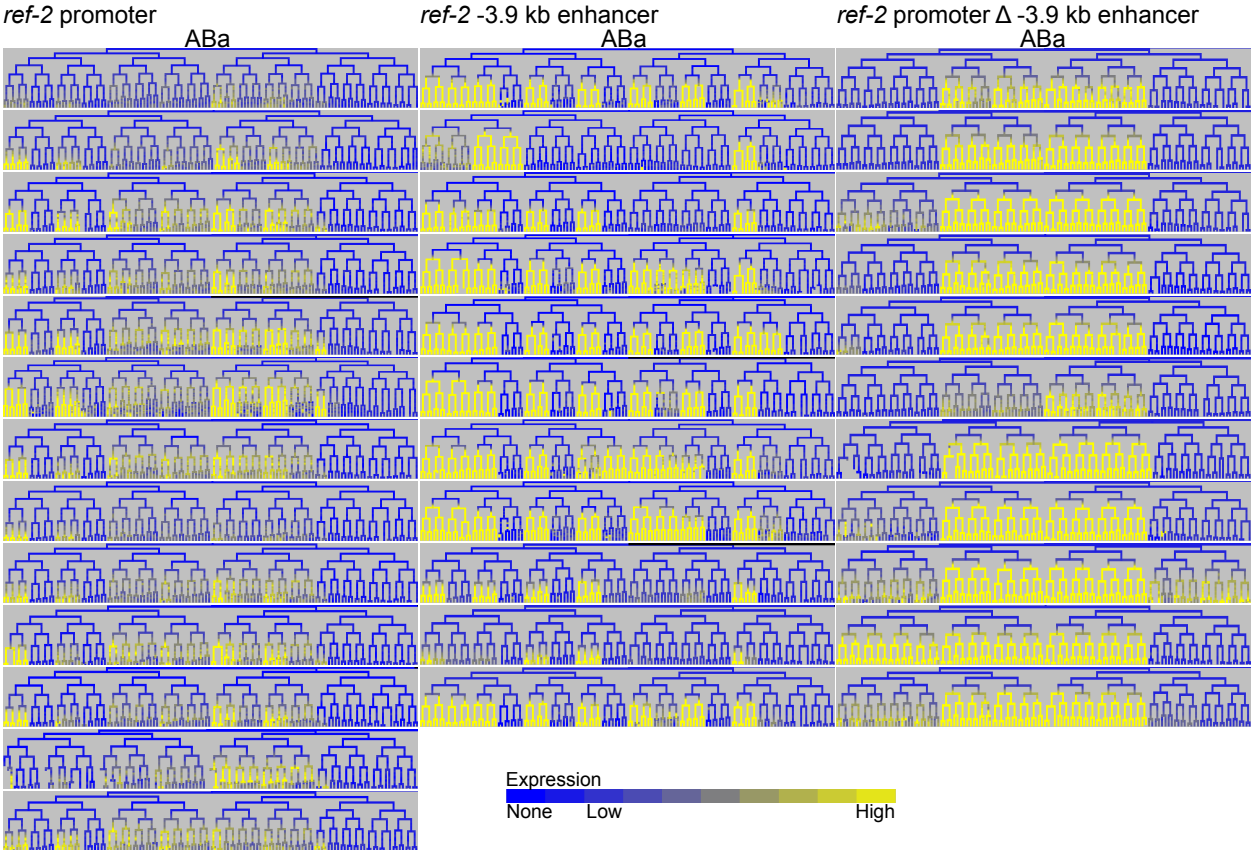

Figure S6: Expression patterns driven by the *ref-2* promoter, the -3.9 kb enhancer, and the promoter lacking the -3.9 kb enhancer are somewhat variable. Displayed here are partial lineages for all analyzed embryos bearing these reporters to show the variation in their expression.

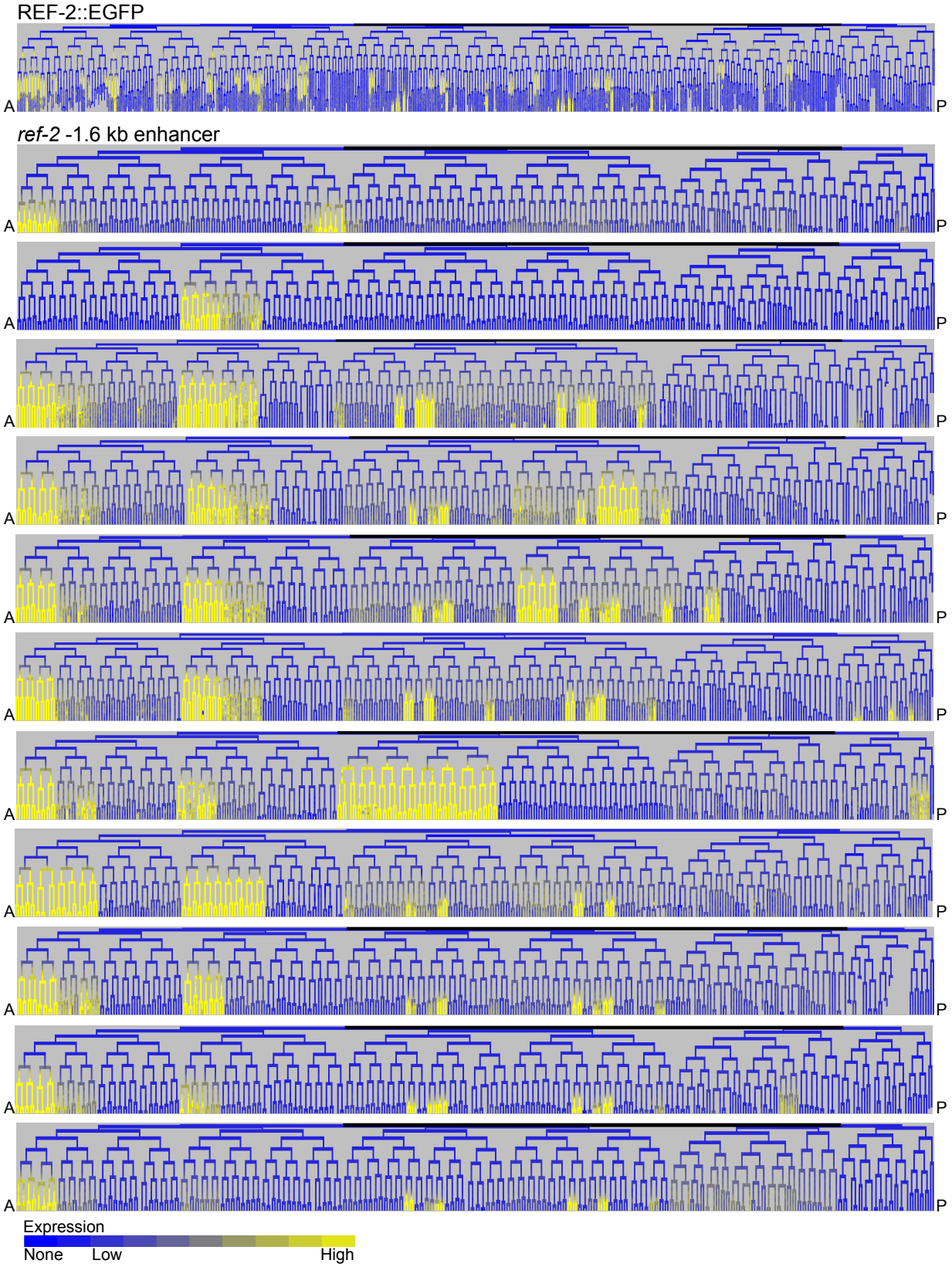
REF-2::EGFP
A
P
ref-2 -1.6 kb enhancer
A
P
A
P
A
P
A
P
A
P
A
P
A
P
A
P
A
P
A
P
A
P
Expression
None
Low
High

Figure S7: Expression patterns driven by the *ref-2* -1.6 kb enhancer are variable. Displayed here are full lineages for all analyzed embryos bearing this reporter to show the variation in its expression.

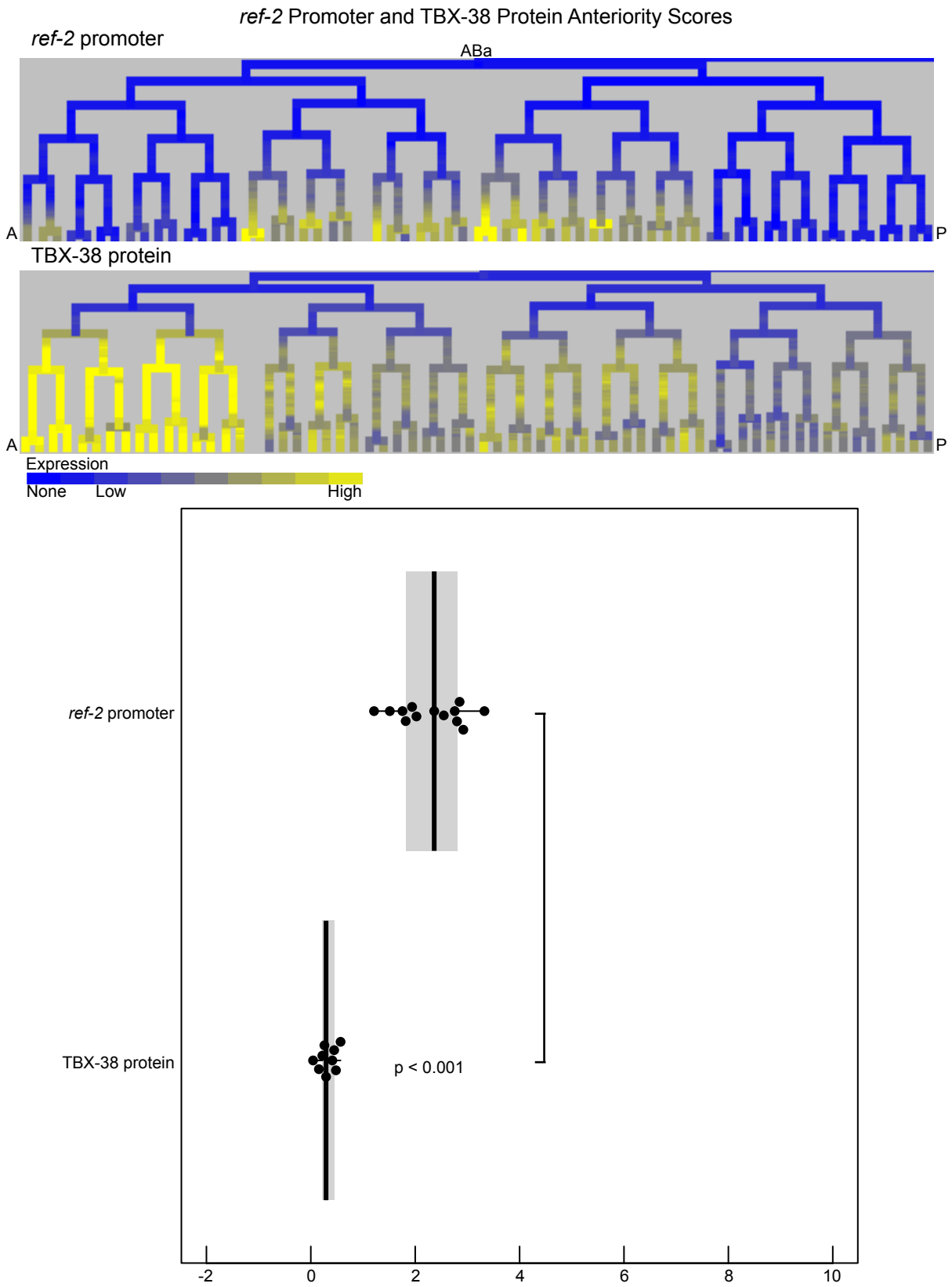
ref-2 Promoter and TBX-38 Protein Anteriority Scores
ref-2 promoter
ABa
A
P
TBX-38 protein
A
P
Expression
None
Low
High
ref-2 promoter
TBX-38 protein
p < 0.001
-2
0
2
4
6
8
10

967 **Figure S8: A TBX-38::GFP CRISPR knock-in protein reporter has minimally anterior-**
968 **biased expression in the lineages in which the *ref-2* promoter drives anterior-biased**
969 **expression.** Displayed are partial lineages of the P*ref-2*::*his-24*::mCherry promoter reporter
970 expression and the TBX-38::GFP CRISPR knock-in expression. The box plot shows the mean
971 anteriority scores for the *ref-2* promoter reporter and the TBX-38::GFP CRISPR knock-in for the
972 same lineages as in Figure 5J.
973
974

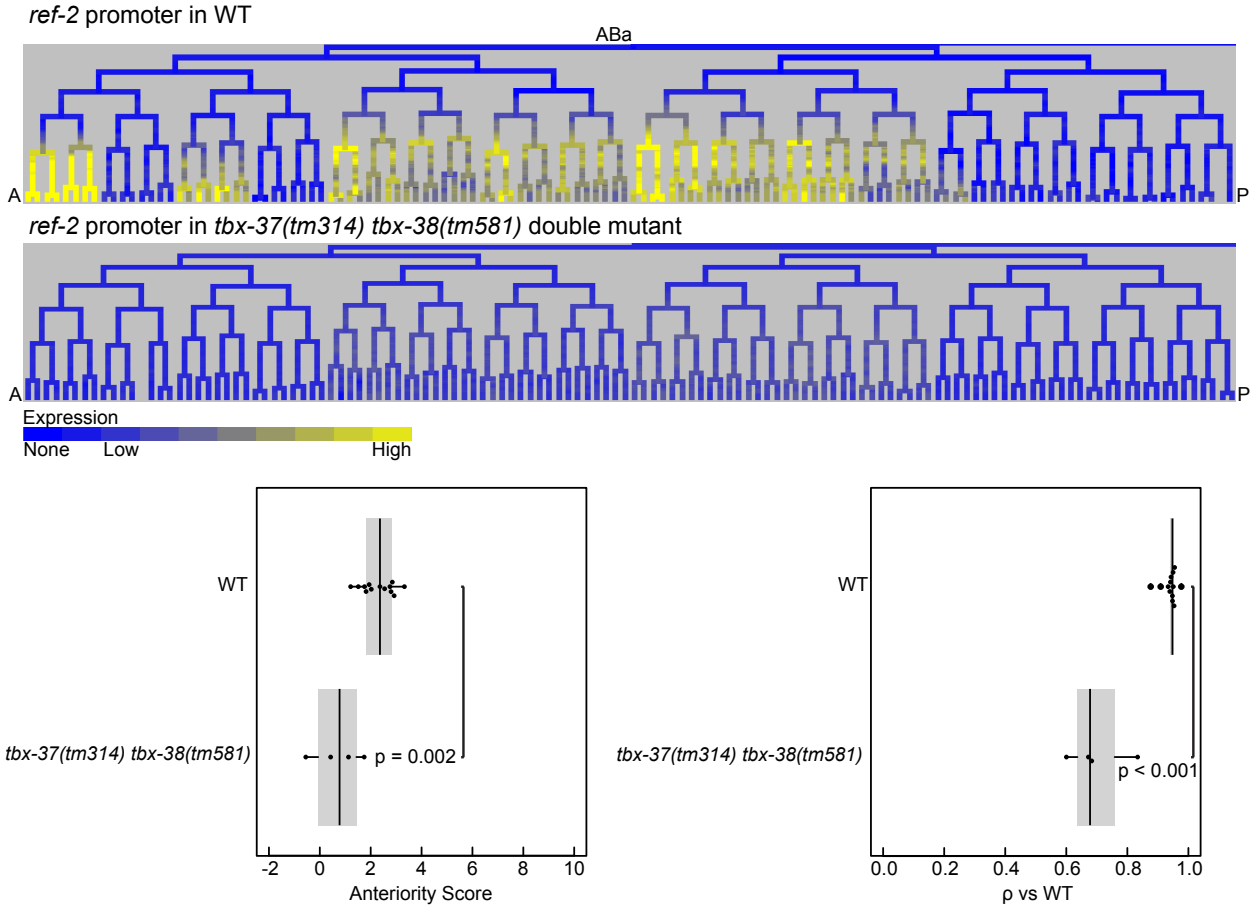

Figure S9: *tbx-37* and *tbx-38* are required for *ref-2* promoter-driven anterior-biased expression in the ABa lineage. Displayed are partial lineages for the expression driven by the *ref-2* promoter in a WT background and in a *tbx-37(tm314) tbx-38(tm581)* double mutant background. Also shown are box plots of anteriority scores and Spearman's ρ for each of these groups, indicating a loss of anterior bias and correlation to WT for the *ref-2* promoter expression pattern in *tbx-37 tbx-38* double mutant embryos. Lineages used to determine anteriority scores are the same as in Figure 5J Spearman's ρ analysis uses the full ABa lineage expression pattern and was calculated relative to the *ref-2* promoter in the WT background.

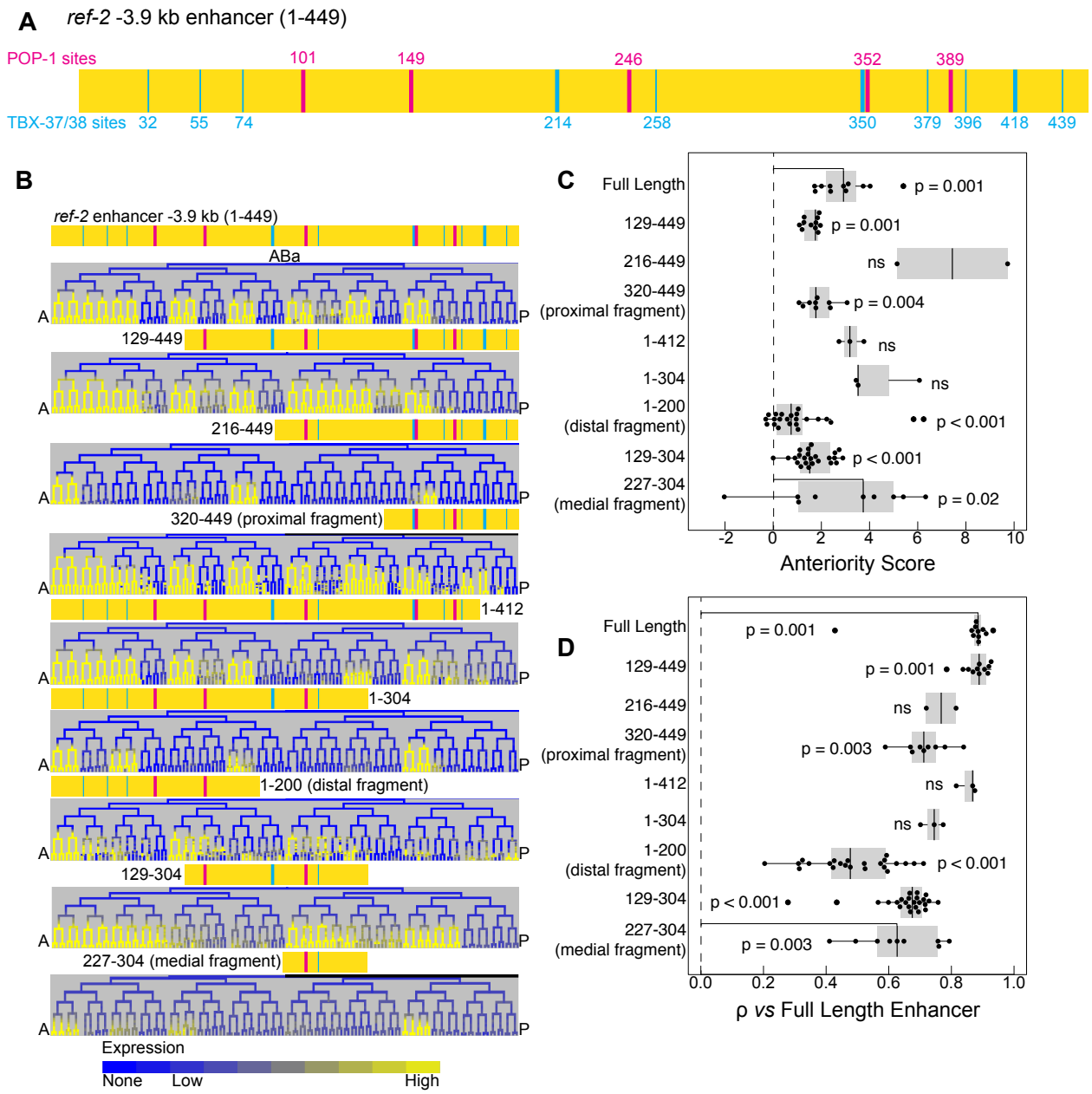

Figure S10: Three non-overlapping fragments of the -3.9 kb enhancer are each sufficient to drive anterior-biased expression in the ABa lineage of the early embryo. A) Model of the *ref-2* -3.9 kb enhancer with predicted TBX-37/38 and POP-1 sites indicated as in Figure 6. B) Expression patterns driven by full-length *ref-2* -3.9 kb enhancer and by all tested fragments. C-D) Box plots displaying the anteriority scores (C) and Spearman's ρ (D) for the full-length *ref-2* -3.9 kb enhancer and all tested fragments. Lineages used to determine anteriority scores are the same as in Figure 5J. Spearman's ρ analysis uses the full ABa lineage and was calculated relative to the full-length -3.9 kb enhancer.

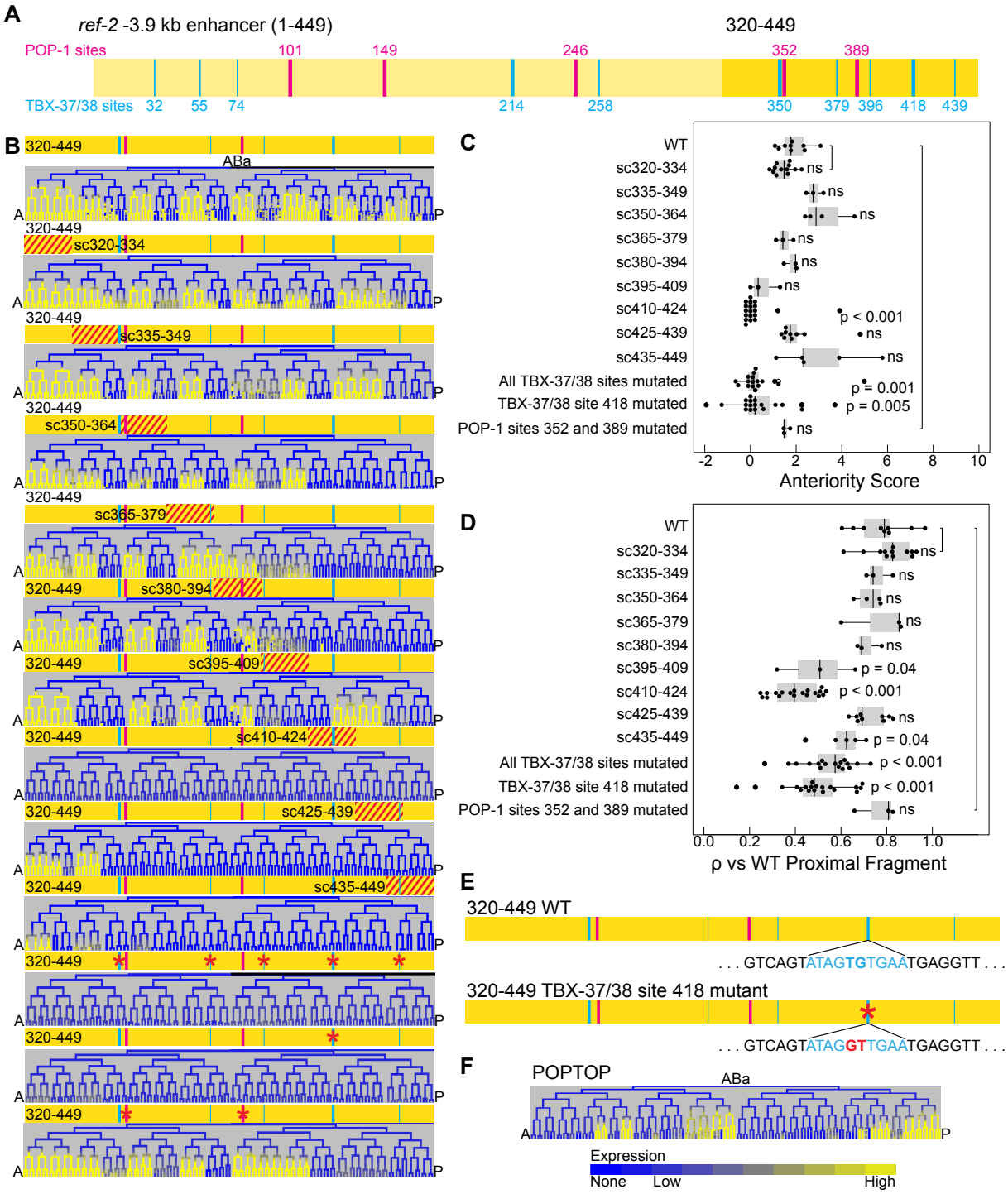

Figure S11: The broadly-expressed transcription factors *tbx-37* and *tbx-38* are required for the anterior-biased expression of *ref-2* in the ABa lineage. A) Model of the *ref-2* -3.9 kb enhancer with proximal fragment (base pairs 320-449) highlighted. Predicted TBX-37/38 and POP-1 sites are indicated as in Figure 6. B) Expression patterns driven by WT proximal fragment of the *ref-2* -3.9 kb enhancer, with each 15 base-pair segment of the fragment scrambled, with all predicted TBX-37/38 sites mutated, with TBX_{418} mutated, and with the two predicted POP-1 sites mutated. C-D) Box plots displaying the anteriority scores (C) and Spearman's ρ (D) for the WT

1005 proximal fragment, with each 15 base-pair segment of the fragment scrambled, with all predicted
1006 TBX-37/38 sites mutated, with *TBX*$_{418}$ mutated, and with the two predicted POP-1 sites mutated.
1007 Lineages used to determine anteriority scores are the same as in Figure 5J. Spearman's ρ analysis
1008 uses the full ABa lineage and was calculated relative to the WT proximal fragment. E) Models of
1009 the proximal fragment of the *ref-2* -3.9 kb enhancer with the WT sequence of *TBX*$_{418}$ and the
1010 mutated sequence used in the *TBX*$_{418}$ mutant reporters. F) Expression pattern driven by the seven-
1011 copy POP-1 site concatemer POPTOP [13, 51].
1012
1013

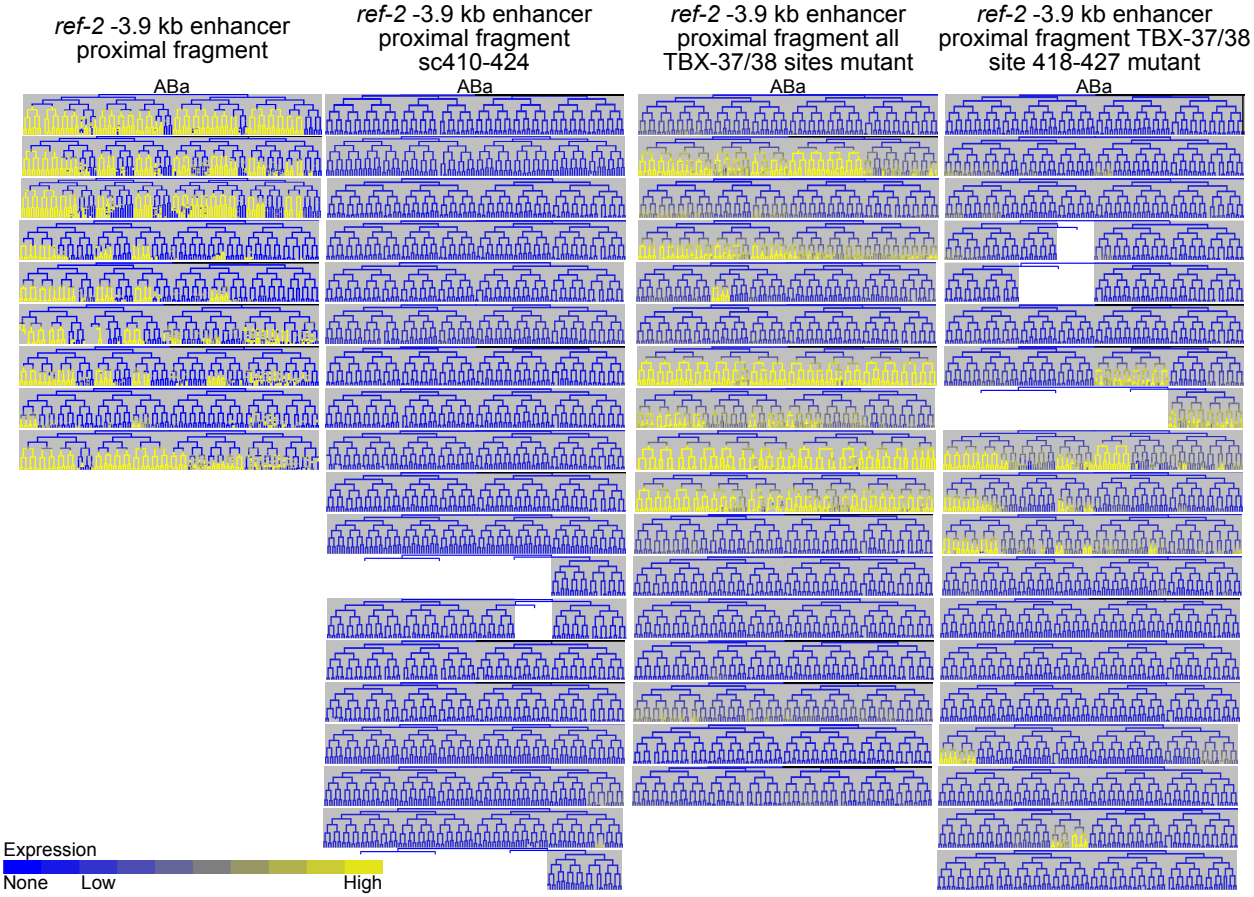

Figure S12: *ref-2* -3.9 kb enhancer WT proximal fragment, proximal fragment with all TBX-37/38 sites mutated, and proximal fragment with *TBX*$_{418}$ mutated exhibit variation in their expression patterns. Displayed are partial lineages for all analyzed embryos expressing reporters for the -3.9 kb enhancer WT proximal fragment, the *ref-2* -3.9 kb enhancer proximal fragment with base pairs 410-424 scrambled, the *ref-2* -3.9 kb enhancer proximal fragment with all TBX-37/38 sites mutated, and the *ref-2* -3.9 kb enhancer proximal fragment with *TBX*$_{418}$ mutated to show the variation in the expression pattern for each of these reporters.

TABLES

Table S1:
Caenorhabditis elegans strain list

Table S2:
Escherichia coli strain list

Table S3:
Quantitative analyses raw data

Table S4:
Anterior gene summary expression data

Table S5:
Recombinant DNA list

ACKNOWLEDGMENTS

We thank J. Archibald Millar for help with data analysis, Julia Richards for collecting and lineaging the PHA-4 movie, and Shaili Patel for her contributions as a laboratory technician. We thank Meera Sundaram for kindly permitting us to use her injection equipment. We thank Jonathan Rumley's PhD thesis committee members for helpful discussions, including committee chair Christopher Brown and committee members Michael Atchison, Peter Klein, Mary Mullins, and Meera Sundaram. Some strains were provided by the CGC, which is funded by NIH Office of Research Infrastructure Programs (P40 OD010440). We also thank the Waterston lab, the Maduro lab, and the Cochella lab for kindly providing us with *C.elegans* strains. We thank the *C. elegans* Reverse Genetics Core Facility at the University of British Columbia, which is part of the international *C. elegans* Gene Knockout Consortium, which produced the *ref-2* mutant allele (*ref-2(gk178))* used in this study. This work was funded by T32GM008216, F31GM123737, and R35GM130357.

1059 **References Cited**

1060 1. Hikasa H, Sokol SY. Wnt signaling in vertebrate axis specification. Cold Spring Harb
1061 Perspect Biol. 2013;5: a007955. doi:10.1101/cshperspect.a007955

1062 2. Archbold HC, Yang YX, Chen L, Cadigan KM. How do they do Wnt they do?: regulation
1063 of transcription by the Wnt/β-catenin pathway. Acta Physiol Oxf Engl. 2012;204: 74–109.
1064 doi:10.1111/j.1748-1716.2011.02293.x

1065 3. Martin BL, Kimelman D. Wnt signaling and the evolution of embryonic posterior
1066 development. Curr Biol CB. 2009;19: R215–R219. doi:10.1016/j.cub.2009.01.052

1067 4. Zacharias AL, Murray JI. Combinatorial decoding of the invariant C. elegans embryonic
1068 lineage in space and time. genesis. 2016;54: 182–197. doi:10.1002/dvg.22928

1069 5. Sulston JE, Schierenberg E, White JG, Thomson JN. The embryonic cell lineage of the
1070 nematode Caenorhabditis elegans. Dev Biol. 1983;100: 64–119. doi:10.1016/0012-
1071 1606(83)90201-4

1072 6. Bürglin TR, Finney M, Coulson A, Ruvkun G. Caenorhabditis elegans has scores of
1073 homoeobox-containing genes. Nature. 1989;341: 239–243. doi:10.1038/341239a0

1074 7. Chen W, Lim HH, Lim L. A new member of the ras superfamily, the rac1 homologue from
1075 Caenorhabditis elegans. Cloning and sequence analysis of cDNA, pattern of developmental
1076 expression, and biochemical characterization of the protein. J Biol Chem. 1993;268: 320–
1077 324. doi:10.1016/S0021-9258(18)54152-1

1078 8. van den Heuvel S. Cell-cycle regulation. WormBook. 2005. pp. 1–16.
1079 doi:10.1895/wormbook.1.28.1

1080 9. Shaye DD, Greenwald I. OrthoList: A Compendium of C. elegans Genes with Human
1081 Orthologs. PLOS ONE. 2011;6: e20085. doi:10.1371/journal.pone.0020085

1082 10. Kim W, Underwood RS, Greenwald I, Shaye DD. OrthoList 2: A New Comparative
1083 Genomic Analysis of Human and Caenorhabditis elegans Genes. Genetics. 2018;210: 445–
1084 461. doi:10.1534/genetics.118.301307

1085 11. Herman M. C. elegans POP-1/TCF functions in a canonical Wnt pathway that controls cell
1086 migration and in a noncanonical Wnt pathway that controls cell polarity. Development.
1087 2001;128: 581–590. doi:10.1242/dev.128.4.581

1088 12. Mizumoto K, Sawa H. Two βs or not two βs: regulation of asymmetric division by β-
1089 catenin. Trends Cell Biol. 2007;17: 465–473. doi:10.1016/j.tcb.2007.08.004

1090 13. Zacharias AL, Walton T, Preston E, Murray JI. Quantitative Differences in Nuclear β-
1091 catenin and TCF Pattern Embryonic Cells in C. elegans. Sternberg PW, editor. PLOS
1092 Genet. 2015;11: e1005585. doi:10.1371/journal.pgen.1005585

1093 14. Lin R, Hill RJ, Priess JR. POP-1 and anterior-posterior fate decisions in C. elegans
1094 embryos. Cell. 1998;92: 229–239.

1095 15. Maduro MF, Lin R, Rothman JH. Dynamics of a developmental switch: recursive
1096 intracellular and intranuclear redistribution of Caenorhabditis elegans POP-1 parallels Wnt-
1097 inhibited transcriptional repression. Dev Biol. 2002;248: 128–142.
1098 doi:10.1006/dbio.2002.0721

1099 16. Huang S, Shetty P, Robertson SM, Lin R. Binary cell fate specification during C. elegans
1100 embryogenesis driven by reiterated reciprocal asymmetry of TCF POP-1 and its
1101 coactivatorβ-catenin SYS-1. Development. 2007;134: 2685–2695. doi:10.1242/dev.008268

1102 17. Calvo D, Victor M, Gay F, Sui G, Po-Shan Luke M, Dufourcq P, et al. A POP-1 repressor
1103 complex restricts inappropriate cell type-specific gene transcription during Caenorhabditis
1104 elegans embryogenesis. EMBO J. 2001;20: 7197–7208. doi:10.1093/emboj/20.24.7197

1105 18. Maduro MF, Kasmir JJ, Zhu J, Rothman JH. The Wnt effector POP-1 and the PAL-
1106 1/Caudal homeoprotein collaborate with SKN-1 to activate C. elegans endoderm
1107 development. Dev Biol. 2005;285: 510–523. doi:10.1016/j.ydbio.2005.06.022

1108 19. Owraghi M, Broitman-Maduro G, Luu T, Roberson H, Maduro MF. Roles of the Wnt
1109 effector POP-1/TCF in the C. elegans endomesoderm specification gene network. Dev Biol.
1110 2010;340: 209–221. doi:10.1016/j.ydbio.2009.09.042

1111 20. Murgan S, Kari W, Rothbächer U, Iché-Torres M, Mélénec P, Hobert O, et al. Atypical
1112 Transcriptional Activation by TCF via a Zic Transcription Factor in C. elegans Neuronal
1113 Precursors. Dev Cell. 2015;33: 737–745. doi:10.1016/j.devcel.2015.04.018

1114 21. Murgan S, Bertrand V. How targets select activation or repression in response to Wnt.
1115 Worm. 2015;4: e1086869. doi:10.1080/21624054.2015.1086869

1116 22. Zhang CU, Blauwkamp TA, Burby PE, Cadigan KM. Wnt-Mediated Repression via
1117 Bipartite DNA Recognition by TCF in the Drosophila Hematopoietic System. Desplan C,
1118 editor. PLoS Genet. 2014;10: e1004509. doi:10.1371/journal.pgen.1004509

1119 23. Sulston JE, Horvitz HR. Post-embryonic cell lineages of the nematode, Caenorhabditis
1120 elegans. Dev Biol. 1977;56: 110–156. doi:10.1016/0012-1606(77)90158-0

1121 24. Murray JI, Boyle TJ, Preston E, Vafeados D, Mericle B, Weisdepp P, et al.
1122 Multidimensional regulation of gene expression in the C. elegans embryo. Genome Res.
1123 2012;22: 1282–1294. doi:10.1101/gr.131920.111

1124 25. Ma X, Zhao Z, Xiao L, Xu W, Kou Y, Zhang Y, et al. A 4D single-cell protein atlas of
1125 transcription factors delineates spatiotemporal patterning during embryogenesis. Nat
1126 Methods. 2021;18: 893–902. doi:10.1038/s41592-021-01216-1

1127 26. Murray JI, Bao Z, Boyle TJ, Boeck ME, Mericle BL, Nicholas TJ, et al. Automated
1128 analysis of embryonic gene expression with cellular resolution in C. elegans. Nat Methods.
1129 2008;5: 703–709. doi:10.1038/nmeth.1228

1130 27. Packer Jonathan S., Zhu Qin, Huynh Chau, Sivaramakrishnan Priya, Preston Elicia, Dueck
1131 Hannah, et al. A lineage-resolved molecular atlas of C. elegans embryogenesis at single-cell
1132 resolution. Science. 2019;365: eaax1971. doi:10.1126/science.aax1971

1133 28. Bao Z, Murray JI, Boyle T, Ooi SL, Sandel MJ, Waterston RH. Automated cell lineage
1134 tracing in Caenorhabditis elegans. Proc Natl Acad Sci U S A. 2006;103: 2707.
1135 doi:10.1073/pnas.0511111103

1136 29. Santella A, Du Z, Nowotschin S, Hadjantonakis A-K, Bao Z. A hybrid blob-slice model for
1137 accurate and efficient detection of fluorescence labeled nuclei in 3D. BMC Bioinformatics.
1138 2010;11: 580. doi:10.1186/1471-2105-11-580

1139 30. Boyle TJ, Bao Z, Murray JI, Araya CL, Waterston RH. AceTree: a tool for visual analysis
1140 of Caenorhabditis elegans embryogenesis. BMC Bioinformatics. 2006;7: 275.
1141 doi:10.1186/1471-2105-7-275

1142 31. Katzman B, Tang D, Santella A, Bao Z. AceTree: a major update and case study in the long
1143 term maintenance of open-source scientific software. BMC Bioinformatics. 2018;19: 121.
1144 doi:10.1186/s12859-018-2127-0

1145 32. Yanai I, Baugh LR, Smith JJ, Roehrig C, Shen-Orr SS, Claggett JM, et al. Pairing of
1146 competitive and topologically distinct regulatory modules enhances patterned gene
1147 expression. Mol Syst Biol. 2008;4. doi:10.1038/msb.2008.6

1148 33. Lin R, Thompson S, Priess JR. pop-1 encodes an HMG box protein required for the
1149 specification of a mesoderm precursor in early C. elegans embryos. Cell. 1995;83: 599–
1150 609. doi:10.1016/0092-8674(95)90100-0

1151 34. Kidd AR, Miskowski JA, Siegfried KR, Sawa H, Kimble J. A β-Catenin Identified by
1152 Functional Rather Than Sequence Criteria and Its Role in Wnt/MAPK Signaling. Cell.
1153 2005;121: 761–772. doi:10.1016/j.cell.2005.03.029

1154 35. Phillips BT, Kidd AR, King R, Hardin J, Kimble J. Reciprocal asymmetry of SYS-1/beta-
1155 catenin and POP-1/TCF controls asymmetric divisions in Caenorhabditis elegans. Proc Natl
1156 Acad Sci. 2007;104: 3231–3236. doi:10.1073/pnas.0611507104

1157 36. Broitman-Maduro G, Owraghi M, Hung WWK, Kuntz S, Sternberg PW, Maduro MF. The
1158 NK-2 class homeodomain factor CEH-51 and the T-box factor TBX-35 have overlapping
1159 function in C. elegans mesoderm development. Dev Camb Engl. 2009;136: 2735–2746.
1160 doi:10.1242/dev.038307

1161 37. Broitman-Maduro G, Lin KT-H, Hung WWK, Maduro MF. Specification of the C. elegans
1162 MS blastomere by the T-box factor TBX-35. Dev Camb Engl. 2006;133: 3097–3106.
1163 doi:10.1242/dev.02475

1164 38. Alper S, Kenyon C. The zinc finger protein REF-2 functions with the Hox genes to inhibit
1165 cell fusion in the ventral epidermis of C. elegans. Development. 2002;129: 3335–3348.
1166 doi:10.1242/dev.129.14.3335

1167 39. Walton T, Preston E, Nair G, Zacharias AL, Raj A, Murray JI. The Bicoid Class
1168 Homeodomain Factors ceh-36/OTX and unc-30/PITX Cooperate in C. elegans Embryonic
1169 Progenitor Cells to Regulate Robust Development. PLOS Genet. 2015;11: e1005003.
1170 doi:10.1371/journal.pgen.1005003

1171 40. Richards JL, Zacharias AL, Walton T, Burdick JT, Murray JI. A quantitative model of
1172 normal Caenorhabditis elegans embryogenesis and its disruption after stress. Dev Biol.
1173 2013;374: 12–23. doi:10.1016/j.ydbio.2012.11.034

1174 41. Maduro MF, Meneghini MD, Bowerman B, Broitman-Maduro G, Rothman JH. Restriction
1175 of Mesendoderm to a Single Blastomere by the Combined Action of SKN-1 and a GSK-3β
1176 Homolog Is Mediated by MED-1 and -2 in C. elegans. Mol Cell. 2001;7: 475–485.
1177 doi:10.1016/S1097-2765(01)00195-2

1178 42. Maduro MF, Hill RJ, Heid PJ, Newman-Smith ED, Zhu J, Priess JR, et al. Genetic
1179 redundancy in endoderm specification within the genus Caenorhabditis. Dev Biol.
1180 2005;284: 509–522. doi:10.1016/j.ydbio.2005.05.016

1181 43. Boeck ME, Boyle T, Bao Z, Murray J, Mericle B, Waterston R. Specific roles for the
1182 GATA transcription factors end-1 and end-3 during C. elegans E-lineage development.
1183 Spec Sect Hist Dev Biol. 2011;358: 345–355. doi:10.1016/j.ydbio.2011.08.002

1184 44. Good K, Ciosk R, Nance J, Neves A, Hill RJ, Priess JR. The T-box transcription factors
1185 TBX-37 and TBX-38 link GLP-1/Notch signaling to mesoderm induction in C. elegans
1186 embryos. Development. 2004;131: 1967–1978. doi:10.1242/dev.01088

1187 45. Andachi Y. Caenorhabditis elegans T-box genes tbx-9 and tbx-8 are required for formation
1188 of hypodermis and body-wall muscle in embryogenesis. Genes Cells. 2004;9: 331–344.
1189 doi:10.1111/j.1356-9597.2004.00725.x

1190 46. Neves A, Priess JR. The REF-1 Family of bHLH Transcription Factors Pattern C. elegans
1191 Embryos through Notch-Dependent and Notch-Independent Pathways. Dev Cell. 2005;8:
1192 867–879. doi:10.1016/j.devcel.2005.03.012

1193 47. Siepel A, Bejerano G, Pedersen JS, Hinrichs AS, Hou M, Rosenbloom K, et al.
1194 Evolutionarily conserved elements in vertebrate, insect, worm, and yeast genomes. Genome
1195 Res. 2005;15: 1034–1050. doi:10.1101/gr.3715005

1196 48. Pollard KS, Hubisz MJ, Rosenbloom KR, Siepel A. Detection of nonneutral substitution
1197 rates on mammalian phylogenies. Genome Res. 2010;20: 110–121.
1198 doi:10.1101/gr.097857.109

1199 49. Kent WJ, Sugnet CW, Furey TS, Roskin KM, Pringle TH, Zahler AM, et al. The Human
1200 Genome Browser at UCSC. Genome Res. 2002;12: 996–1006. doi:10.1101/gr.229102

1201 50. Charest J, Daniele T, Wang J, Bykov A, Mandlbauer A, Asparuhova M, et al.
1202 Combinatorial Action of Temporally Segregated Transcription Factors. Dev Cell. 2020;55:
1203 483-499.e7. doi:10.1016/j.devcel.2020.09.002

1204 51. LaBonty M, Szmygiel C, Byrnes LE, Hughes S, Woollard A, Cram EJ. CACN-1/Cactin
1205 plays a role in Wnt signaling in C. elegans. PloS One. 2014;9.
1206 doi:10.1371/journal.pone.0101945

1207 52. Murray JI, Preston E, Crawford JP, Rumley JD, Amom P, Anderson BD, et al. The anterior
1208 Hox gene ceh-13 and elt-1/GATA activate the posterior Hox genes

1209 nob-1 and php-3 to specify posterior lineages in the C.
1210 elegans embryo. bioRxiv. 2021; 2021.02.09.430385. doi:10.1101/2021.02.09.430385

1211 53. Poole RJ, Hobert O. Early Embryonic Programming of Neuronal Left/Right Asymmetry in
1212 C. elegans. Curr Biol. 2006;16: 2279–2292. doi:10.1016/j.cub.2006.09.041

1213 54. Rocheleau CE, Yasuda J, Shin TH, Lin R, Sawa H, Okano H, et al. WRM-1 Activates the
1214 LIT-1 Protein Kinase to Transduce Anterior/Posterior Polarity Signals in C. elegans. Cell.
1215 1999;97: 717–726. doi:10.1016/S0092-8674(00)80784-9

1216 55. Lo M-C, Gay F, Odom R, Shi Y, Lin R. Phosphorylation by the β-Catenin/MAPK Complex
1217 Promotes 14-3-3-Mediated Nuclear Export of TCF/POP-1 in Signal-Responsive Cells in C.
1218 elegans. Cell. 2004;117: 95–106. doi:10.1016/S0092-8674(04)00203-X

1219 56. Kaletta T, Schnabel H, Schnabel R. Binary specification of the embryonic lineage in
1220 Caenorhabditis elegans. Nature. 1997;390: 294–298. doi:10.1038/36869

1221 57. Fukushige T, Brodigan TM, Schriefer LA, Waterston RH, Krause M. Defining the
1222 transcriptional redundancy of early bodywall muscle development in C. elegans: evidence
1223 for a unified theory of animal muscle development. Genes Dev. 2006;20: 3395–3406.
1224 doi:10.1101/gad.1481706

1225 58. Fukushige T, Krause M. The myogenic potency of HLH-1 reveals wide-spread
1226 developmental plasticity in early C. elegans embryos. Dev Camb Engl. 2005;132: 1795–
1227 1805. doi:10.1242/dev.01774

1228 59. Simonis N, Rual J-F, Carvunis A-R, Tasan M, Lemmens I, Hirozane-Kishikawa T, et al.
1229 Empirically controlled mapping of the Caenorhabditis elegans protein-protein interactome
1230 network. Nat Methods. 2009;6.

1231 60. Tintori SC, Osborne Nishimura E, Golden P, Lieb JD, Goldstein B. A Transcriptional
1232 Lineage of the Early C. elegans Embryo. Dev Cell. 2016;38: 430–444.
1233 doi:10.1016/j.devcel.2016.07.025

1234 61. Whiting J, Marshall H, Cook M, Krumlauf R, Rigby PW, Stott D, et al. Multiple spatially
1235 specific enhancers are required to reconstruct the pattern of Hox-2.6 gene expression.
1236 Genes Dev. 1991;5: 2048–2059. doi:10.1101/gad.5.11.2048

1237 62. Epstein DJ, McMahon AP, Joyner AL. Regionalization of Sonic hedgehog transcription
1238 along the anteroposterior axis of the mouse central nervous system is regulated by Hnf3-
1239 dependent and -independent mechanisms. Development. 1999;126: 281–292.
1240 doi:10.1242/dev.126.2.281

1241 63. Teng Y, Girard L, Ferreira HB, Sternberg PW, Emmons SW. Dissection of cis-regulatory
1242 elements in the C. elegans Hox gene egl-5 promoter. Dev Biol. 2004;276: 476–492.
1243 doi:10.1016/j.ydbio.2004.09.012

1244 64. Streit A, Kohler R, Marty T, Belfiore M, Takacs-Vellai K, Vigano M-A, et al. Conserved
1245 Regulation of the Caenorhabditis elegans labial/Hox1 Gene ceh-13. Dev Biol. 2002;242:
1246 96–108. doi:10.1006/dbio.2001.0544

1247 65. Landmann F, Quintin S, Labouesse M. Multiple regulatory elements with spatially and
1248 temporally distinct activities control the expression of the epithelial differentiation gene lin-
1249 26 in C. elegans. Dev Biol. 2004;265: 478–490. doi:10.1016/j.ydbio.2003.09.009

1250 66. Chen RA-J, Down TA, Stempor P, Chen QB, Egelhofer TA, Hillier LW, et al. The
1251 landscape of RNA polymerase II transcription initiation in C. elegans reveals promoter and
1252 enhancer architectures. Genome Res. 2013;23: 1339–1347. doi:10.1101/gr.153668.112

1253 67. Serizay J, Dong Y, Jänes J, Chesney M, Cerrato C, Ahringer J. Distinctive regulatory
1254 architectures of germline-active and somatic genes in C. elegans. Genome Res. 2020;30:
1255 1752–1765. doi:10.1101/gr.265934.120

1256 68. Bertrand V, Hobert O. Linking asymmetric cell division to the terminal differentiation
1257 program of postmitotic neurons in C. elegans. Dev Cell. 2009;16: 563–575.
1258 doi:10.1016/j.devcel.2009.02.011

1259 69. Kuersten S, Segal SP, Verheyden J, LaMartina SM, Goodwin EB. NXF-2, REF-1, and
1260 REF-2 Affect the Choice of Nuclear Export Pathway for tra-2 mRNA in C. elegans. Mol
1261 Cell. 2004;14: 599–610. doi:10.1016/j.molcel.2004.05.004

1262 70. Clark E, Akam M. Odd-paired controls frequency doubling in Drosophila segmentation by
1263 altering the pair-rule gene regulatory network. Wittkopp PJ, editor. eLife. 2016;5: e18215.
1264 doi:10.7554/eLife.18215

1265 71. Yoon Y, Klomp J, Martin-Martin I, Criscione F, Calvo E, Ribeiro J, et al. Embryo polarity
1266 in moth flies and mosquitoes relies on distinct old genes with localized transcript isoforms.
1267 Wittkopp PJ, Pick L, Popadic A, Akam M, editors. eLife. 2019;8: e46711.
1268 doi:10.7554/eLife.46711

1269 72. Kamath RS, Fraser AG, Dong Y, Poulin G, Durbin R, Gotta M, et al. Systematic functional
1270 analysis of the Caenorhabditis elegans genome using RNAi. Nature. 2003;421: 231–237.
1271 doi:10.1038/nature01278

1272 73. Vora S, Phillips BT. Centrosome-Associated Degradation Limits β-Catenin Inheritance by
1273 Daughter Cells after Asymmetric Division. Curr Biol. 2015;25: 1005–1016.
1274 doi:10.1016/j.cub.2015.02.020

1275 74. Weirauch MT, Yang A, Albu M, Cote AG, Montenegro-Montero A, Drewe P, et al.
1276 Determination and inference of eukaryotic transcription factor sequence specificity. Cell.
1277 2014;158: 1431–1443. doi:10.1016/j.cell.2014.08.009

1278 75. Narasimhan K, Lambert SA, Yang AWH, Riddell J, Mnaimneh S, Zheng H, et al. Mapping
1279 and analysis of transcription factor sequence specificities. eLife. 2015;4.
1280 doi:10.7554/eLife.06967

1281 76. Bao Z, Murray JI. Mounting Caenorhabditis elegans Embryos for Live Imaging of
1282 Embryogenesis. Cold Spring Harb Protoc. 2011;2011: pdb.prot065599.
1283 doi:10.1101/pdb.prot065599